

Black holes in dS_3

Roberto Emparan,^{1,2} Juan F. Pedraza,³ Andrew Svesko,⁴ Marija Tomašević,⁵ and
Manus R. Visser⁶

¹*Institució Catalana de Recerca i Estudis Avançats (ICREA)
Passeig Lluis Companys, 23, 08010 Barcelona, Spain*

²*Departament de Física Quàntica i Astrofísica and Institut de Ciències del Cosmos,
Universitat de Barcelona, 08028 Barcelona, Spain*

³*Instituto de Física Teórica UAM/CSIC
Calle Nicolás Cabrera 13-15, Cantoblanco, 28049 Madrid, Spain*

⁴*Department of Physics and Astronomy, University College London,
Gower Street, London, WC1E 6BT, United Kingdom*

⁵*Centre de Physique Théorique (CPHT), Ecole Polytechnique,
Bâtiment 6, Route de Saclay, 91128 Palaiseau, Cedex, France*

⁶*University of Geneva, Department of Theoretical Physics
24 quai Ernest-Ansermet, 1211 Genève 4, Switzerland*

E-mail: emparan@ub.edu, j.pedraza@csic.es, a.svesko@ucl.ac.uk,
marija.tomasevic@polytechnique.edu, manus.visser@unige.ch

ABSTRACT: In three-dimensional de Sitter space classical black holes do not exist, and the Schwarzschild-de Sitter solution instead describes a conical defect with a single cosmological horizon. We argue that the quantum backreaction of conformal fields can generate a black hole horizon, leading to a three-dimensional quantum de Sitter black hole. Its size can be as large as the cosmological horizon in a Nariai-type limit. We show explicitly how these solutions arise using braneworld holography, but also compare to a non-holographic, perturbative analysis of backreaction due to conformally coupled scalar fields in conical de Sitter space. We analyze the thermodynamics of this quantum black hole, revealing it behaves similarly to its classical four-dimensional counterpart, where the generalized entropy replaces the classical Bekenstein-Hawking entropy. We compute entropy deficits due to nucleating the three-dimensional black hole and revisit arguments for a possible matrix model description of dS spacetimes. Finally, we comment on the holographic dual description for dS spacetimes as seen from the braneworld perspective.

Contents

1	Introduction	1
2	Perturbative backreaction of quantum fields in conical dS_3	6
3	de Sitter braneworld in AdS_4	8
4	Quantum Schwarzschild-de Sitter black hole	12
4.1	AdS ₄ C-metric	12
4.2	Black hole on the brane	15
4.3	Nariai Limit	16
4.4	Solution parameters and validity range: 4D and 3D views	18
4.5	Backreaction and quantum black holes	19
5	Thermodynamics of the quantum SdS black hole	23
6	Entropy deficit and nucleation rate of quantum dS black holes	31
6.1	Entropy deficit	32
6.2	Nucleation rate	34
7	Comments on the holographic dual of de Sitter	37
8	Conclusion	41
A	Gravitational attraction from negative energy	44
B	Renormalized stress tensor of conical defect in dS_3	45
C	Bulk dual of a CFT in conical dS_3	49
D	Entropy deficit of small quantum dS black hole	50

1 Introduction

Three-dimensional black holes, lost and found. Lowering the dimensionality of spacetime simplifies the study of gravity, but often at a hefty price: black holes are wont to depart the scene. This follows from simple dimensional arguments. In three spacetime dimensions, which will be the focus of this article, if we can only use Newton's constant G_3 , then the presence of a massive object does not by itself introduce any length scale, since $G_3 M$ is a

dimensionless quantity.¹ Therefore, there cannot be any black hole horizon solely determined by the mass of an object. Instead, the gravitational effect of a particle coupled to gravity becomes manifest only as a scale-free conical deficit [1].

A cosmological constant can remedy this and allow black holes with a size proportional to the radius of three-dimensional Anti-de Sitter (AdS) space [2, 3]. However, although a length scale is necessary to have a horizon, it is not sufficient: some form of gravitational attraction is also needed. The tendency to collapse in AdS does it, but in de Sitter (dS) space the effect goes the other way around, and only a cosmological horizon, not a black hole, results from the cosmological length scale. Explicitly, in dS₃ with cosmological constant $\Lambda_3 = 1/R_3^2$, the geometry for a particle of mass M at the pole is, in static coordinates [4],

$$ds^2 = -f(r)dt^2 + f^{-1}(r)dr^2 + r^2d\phi^2, \quad f(r) = 1 - 8G_3M - \frac{r^2}{R_3^2}. \quad (1.1)$$

This contains a conical singularity at $r = 0$, with deficit angle

$$\delta = 2\pi \left(1 - \sqrt{1 - 8G_3M}\right), \quad (1.2)$$

and no black hole. In fact, since constant time slices in dS₃ are two-spheres, globally there are two conical singularities in the maximal extension of (1.1), one at every pole of the two-sphere.

A more subtle way of introducing a length scale is via quantum effects: with $\hbar \neq 0$, the Planck length

$$L_P = \hbar G_3 \quad (1.3)$$

makes an appearance.² But even before knowing how this scale may enter to yield black holes, one may fear that it will fail to do so in a sensible way. If the black hole size must be proportional to the Planck length, then quantum gravitational effects might render the semi-classical description unreliable. To understand that this need not be so, note, first, that the presence of $\hbar G_3$ in this discussion does not immediately imply that quantum gravity must be important, but only that both gravitational and quantum effects are at play, *e.g.*, with quantum fields coupled to classical gravity. When a large number $c \gg 1$ of these fields are introduced, the energy of their combined quantum effects, $\propto c\hbar$, may gravitate to give rise to a large semi-classical black hole horizon of radius $\sim G_3c\hbar = cL_P \gg L_P$, near which quantum gravity effects would be relatively small. In the limit where $c \rightarrow \infty$ and $L_P \rightarrow 0$ with cL_P fixed, such effects are absent, while the classical gravitational backreaction of the quantum fields remains finite. It is then conceivable that this backreaction results in a black hole of radius $\sim cL_P$.^{3,4} Interestingly, its Bekenstein-Hawking entropy will then be $\sim c$, with no factors of \hbar , which indicates that it originates from microscopic one-loop effects in quantum field theory.

¹We always set the speed of light equal to one.

²In contrast, there is no notion of a three-dimensional Planck mass.

³In all dimensions, classical Einstein gravity coupled to scale-invariant matter (quantum or classical) is itself a scale-invariant theory, such that in the setup described one can always choose units where $cL_P = 1$.

⁴The large number of fields also lowers the cutoff energy scale of the quantum theory down to $1/(cL_P)$. The consequences in this context were discussed in [5] and will be reviewed later below.

Quantum backreaction. This mechanism was realized in [5] to obtain black holes in three-dimensional asymptotically locally flat space, as well as AdS₃ black holes with masses lower than the BTZ black holes (see also [6]). Here we will employ it in three-dimensional de Sitter space. It can be convenient to envisage it as a two-step process. First, one solves for a quantum field in the spacetime (1.1). The conical periodicity conditions give rise to a Casimir effect. For a free conformal scalar, we find that this results in a renormalized stress tensor of the form

$$\langle T^\mu{}_\nu \rangle = \frac{F(M)}{8\pi r^3} \text{diag}(1, 1, -2), \quad (1.4)$$

with $F(M) > 0$. Therefore, the Casimir energy density in (1.4) is negative, but when, in the next step, we compute its backreaction on the geometry, we find

$$\delta g_{tt} = \frac{2L_P F(M)}{r} > 0, \quad (1.5)$$

which means that the gravitational effect is attractive [7, 8].⁵ Then, if a large number of fields are present, a semi-classical black hole horizon may appear. To prove this, the backreaction of the large number of fields must be non-linearly accounted for, that is, one must simultaneously solve the quantum field and the gravitational equations. The only framework that we know of where this can be consistently done in three or more dimensions is braneworld holography.

In this setup, classical dynamics in an AdS_{*d*+1} bulk with a *d*-dimensional brane holographically encodes the quantum dynamics of the dual *d*-dimensional conformal field theory coupled to a *d*-dimensional gravitational theory on the brane. In our context, the semi-classical Einstein equations in a four-dimensional AdS bulk are recast in the three-dimensional form

$$G_{\mu\nu} + \frac{1}{R_3^2} g_{\mu\nu} + \dots = 8\pi G_3 \langle T_{\mu\nu} \rangle, \quad (1.6)$$

where $g_{\mu\nu}$ is the metric induced on the brane, with curvature radius R_3 and Einstein tensor $G_{\mu\nu}$, and the dots denote higher curvature terms which can be systematically computed order by order [6, 9]. These can be regarded, in dual terms, as induced by integrating out the holographic CFT degrees of freedom above the ultraviolet cutoff that the brane represents. The CFT below this cutoff gives rise to a renormalized $\langle T_{\mu\nu} \rangle$, with a large central charge $c \gg 1$ given by the AdS₄ radius in four-dimensional Planck units. Crucially, the bulk solution exactly encodes the quantum backreaction of the CFT on the three-dimensional geometry.

Quantum black hole in dS₃. In this article, we apply this holographic approach to obtain black holes from quantum backreaction in three-dimensional de Sitter space. As in [5, 6], we use an exact solution of a black hole in an AdS₄ braneworld, but now with a brane with large enough tension such that the effective cosmological constant on the brane is positive.⁶

⁵Briefly, the reason is the following. A region of localized negative energy has a repulsive effect in its exterior, but the more one enters the region, the less repulsion is felt. As a result, at finite r there is an effective attraction from the energy in (1.4). We elaborate on this explanation in Appendix A.

⁶A black hole solution was found in [10] for a massive gravity theory in dS₃. Although the “new massive gravity” action of that article contains a term of the same form as the quadratic curvature term in our brane effective action, the two theories differ, and in particular our theory of gravity in dS₃ is not massive.

Using this solution, we find that the holographic non-linear backreaction changes the conical geometry (1.1) to have

$$f(r) = 1 - 8G_3M - \frac{r^2}{R_3^2} - \frac{2cL_P F(M)}{r}. \quad (1.7)$$

It is easy to verify that the quantum $1/r$ term gives rise to a black hole horizon. This “quantum Schwarzschild-dS₃” (qSdS) solution is exact to all orders in the backreaction, in the planar limit of the CFT. The corrections are proportional to the central charge c of the CFT, and the function $F(M)$ is now obtained by demanding regularity of the four-dimensional bulk. It differs from that of free scalars in (1.4), where $c = 1$, but the radial $1/r$ dependence (which is natural from the four-dimensional holographic perspective) and the tensorial structure of the corrections are the same in both cases.

Observe also that the physical range of masses in the conical spacetime (1.1) is bounded above,

$$0 < M < \frac{1}{8G_3}, \quad (1.8)$$

with the maximum mass reached when the conical deficit eats up all the space. The mass of the black holes in (1.7) is also bounded above, but now the effect is due to the black hole horizon becoming as large as the cosmological horizon. This is a Nariai limit [11, 12] analogous to the one in Schwarzschild-de Sitter solutions in $d \geq 4$, and it gives an upper mass bound that is lower (or equal) compared to (1.1). Since this limit is due to the appearance of the $1/r$ term in the metric, we expect that it is not exclusive of the holographic construction, but instead a generic property of quantum black holes in dS₃.

Thermodynamics. A central focus of this article is the thermodynamics of the quantum black hole. This depends on the specific form of $F(M)$, so our results for the horizon entropies are dependent on the holographic realization of the solution, but the form of the first laws below is expected to hold generically for semi-classical de Sitter gravity.

From the bulk perspective, the classical four-dimensional Bekenstein-Hawking entropy of each horizon is holographically understood to be the generalized entropy $S_{\text{gen}}^{(3)}$ in three dimensions [6, 13]. The separation of the high- and low-energy CFT degrees of freedom also delimit the generalized entropy into the Wald entropy S_{Wald} (accounting for higher curvature corrections), and entanglement entropy S_{out} generated by the CFT living outside of each horizon,

$$S_{\text{gen}}^{(3)} = S_{\text{Wald}} + S_{\text{out}}. \quad (1.9)$$

Further, each horizon of the quantum Schwarzschild-de Sitter black hole obeys a first law of thermodynamics,

$$dM = T_h dS_{\text{gen},h}^{(3)}, \quad dM = -T_c dS_{\text{gen},c}^{(3)}, \quad (1.10)$$

where $T_{h,c} = \frac{\kappa_{h,c}}{2\pi}$ refers to the Gibbons-Hawking temperature of the two horizons, with surface gravities $\kappa_{h,c}$ defined with respect to the time translation Killing vector ∂_t , and M is the mass. Importantly, the generalized entropy is an exact classical four-dimensional quantity,

while the mass M , and temperatures $T_{c,h}$ are all three-dimensional quantities measured on the brane. Thence, as with the first law of the quantum BTZ black hole [6], the first laws (1.10) represent a non-trivial test of braneworld holography. Adding the two first laws yields

$$0 = T_h dS_{\text{gen},h}^{(3)} + T_c dS_{\text{gen},c}^{(3)}, \quad (1.11)$$

a three-dimensional analog of the semi-classical first law in dS_2 explored in [14],⁷ and a semi-classical generalization of the usual first law of higher dimensional SdS black holes [15]. Notably, the first laws (1.10) and (1.11) hold to all orders in backreaction and higher curvature corrections.

Outline. This article is structured as follows. In Sec. 2 we consider a massless scalar field conformally coupled in a conical dS_3 background and derive the quantum corrected geometry perturbatively. In Sec. 3 we describe the bulk AdS_4 geometry including a brane with a dS_3 slicing. We briefly review the gravitational theory induced on the brane, and uncover the semi-classical gravitational equations of motion, at least to second order in the strength of backreaction. Sec. 4 is devoted to finding the black hole solution localized on the brane, which is interpreted as the quantum three-dimensional Schwarzschild-de Sitter black hole. We also detail the Nariai limit of the qSdS solution, which is nearly identical to the Nariai limit of the classical four-dimensional SdS black hole. In Sec. 5 we analyze the thermodynamics of the quantum black hole. We find the three-dimensional thermodynamic quantities $S_{\text{gen}}^{(3)}$, T , and M behave similar to their classical four-dimensional counterparts. In Sec. 6, we compute the entropy deficit between the *generalized* entropies of the dS_3 and the qSdS₃ horizons surrounded by a CFT, which extend arguments hinting at a matrix model description of dS spacetimes and are also used to calculate the nucleation rate of a (quantum) black hole appearing in dS_3 . In Sec. 7 we comment on a possible realization of dS/CFT which naturally arises from holographic braneworlds. We conclude in Sec. 8, where we outline multiple future research avenues.

To keep this article self-contained we include multiple appendices. In App. A we explain how the negative Casimir energy generated by a conical defect leads to an attractive gravitational potential. In App. B we provide the computational details of the quantum backreaction due to a massless conformally coupled scalar field in a dS_3 conical defect background. App. C shows that in the limit of zero backreaction the AdS_4 bulk geometry is equal to the hyperbolic AdS_4 black hole upon a double Wick rotation. App. D provides computational details of the entropy deficit of quantum de Sitter black holes.

⁷In the two-dimensional context the generalized entropy arises from including the 1-loop Polyakov action to describe the backreaction effects of a two-dimensional (not necessarily holographic) CFT.

2 Perturbative backreaction of quantum fields in conical dS₃

Consider a massless scalar field Φ conformally coupled to Einstein gravity in three dimensions,

$$I = \frac{1}{16\pi G_3} \int d^3x \sqrt{-g} [R - 2\Lambda] - \frac{1}{2} \int d^3x \sqrt{-g} \left[(\nabla\Phi)^2 + \frac{1}{8} R\Phi^2 \right]. \quad (2.1)$$

We are interested in the renormalized stress-energy tensor of the field in the geometry (1.1) of a conical defect in dS₃. It can be computed using a method analogous to that of the AdS₃ case in [16], and here we only sketch it, deferring the details to App. B.

Generically, the Green's function for the scalar field equation in dS₃ is

$$G(x, x') = \frac{1}{4\pi} \frac{1}{|x - x'|} + \frac{\lambda}{4\pi} \frac{1}{|x + x'|}, \quad (2.2)$$

where $|x - x'| \equiv \sqrt{(x - x')^a (x - x')_a}$ is the chordal or geodesic distance between x and x' in the four-dimensional embedding space $\mathbb{R}^{2,2}$. The parameter λ corresponds to different boundary conditions imposed on $G(x, x')$, namely ‘transparent’ ($\lambda = 0$), Neumann ($\lambda = 1$), or Dirichlet ($\lambda = -1$) boundary conditions [17, 18]. We will focus on the case of transparent boundary conditions. These are analogous to the definition in AdS₃, where they correspond to the case where the scalar field modes defined with respect to the time translation Killing vector are smooth on the Einstein static universe, obtained from an appropriate conformal transformation of dS₃. The holographic approach that we will employ later naturally selects these conditions too.

If we consider that the conical spacetime is a \mathbb{Z}_N orbifold, then the Green's function in it can be computed by summing over the N images under the discrete action of ∂_ϕ . With that, the renormalized quantum stress tensor $\langle T_{\mu\nu} \rangle$ can be derived by appropriately taking point-split derivatives, and a finite result is obtained after subtracting the ‘vacuum’ term. After all this is done, we find a stress tensor of the form (1.4), with

$$F(M) = \hbar \frac{\gamma^3}{4\sqrt{2}} \sum_{n=1}^{N-1} \frac{3 + \cos(2\pi n\gamma)}{[1 - \cos(2\pi n\gamma)]^{3/2}}, \quad (2.3)$$

where the parameter

$$\gamma = \sqrt{1 - 8G_3 M} \quad (2.4)$$

is related to the deficit angle (1.2) as $\delta = 2\pi(1 - \gamma)$.

We can now compute the gravitational effect of this stress-energy by coupling it to the Einstein equations

$$G^\mu_\nu + \frac{1}{R_3^2} \delta^\mu_\nu = 8\pi G_3 \langle T^\mu_\nu \rangle, \quad (2.5)$$

and solving these perturbatively in $G_3 \hbar = L_P$ around the conical defect metric (1.1). Analogous to the computation of quantum backreaction in conical AdS₃ [19, 20], we consider a

static and circularly symmetric background with the metric ansatz in circle-radius gauge, such that $g_{\phi\phi} = r^2$,

$$ds^2 = -A(r)dt^2 + B(r)dr^2 + r^2d\phi^2 . \quad (2.6)$$

The tt , rr and $\phi\phi$ components of the semi-classical Einstein equations (2.5) are, respectively,

$$\begin{aligned} -\frac{B'}{2rB^2} + \frac{1}{R_3^2} &= \frac{L_P F(M)}{r^3} , \\ \frac{A'}{2rAB} + \frac{1}{R_3^2} &= \frac{L_P F(M)}{r^3} , \\ \frac{2ABA'' - AA'B' - BA'^2}{4A^2B^2} + \frac{1}{R_3^2} &= -2\frac{L_P F(M)}{r^3} . \end{aligned} \quad (2.7)$$

The general solution for A and B will depend on two integration constants, one of which is set to unity upon reparameterizing the time coordinate. The quantum effects must be regarded as a perturbation around the conical spacetime, so we must solve the equations as

$$A = 1 - 8G_3M - \frac{r^2}{R_3^2} - \gamma_{tt}(r) , \quad (2.8)$$

$$B = \frac{1}{1 - 8G_3M - \frac{r^2}{R_3^2} - \gamma_{rr}(r)} = \frac{1}{1 - 8G_3M - \frac{r^2}{R_3^2}} \left(1 + \frac{\gamma_{rr}(r)}{1 - 8G_3M - \frac{r^2}{R_3^2}} + \mathcal{O}(L_P)^2 \right) , \quad (2.9)$$

with $\gamma_{tt}(r)$ and $\gamma_{rr}(r)$ quantities of first order in L_P . Solving the equations to this order gives

$$\gamma_{tt} = \gamma_{rr} = \frac{2L_P F(M)}{r} . \quad (2.10)$$

The fact that $\gamma_{tt} > 0$ indicates an attractive gravitational effect, which suggest that a black hole horizon might form where $\gamma_{tt} \approx 1 - 8G_3M - r^2/R_3^2$. Of course, the perturbative nature of this solution does not entitle us to definitively reach this conclusion, but it is worth noticing that if we write the backreacted metric in the form

$$ds^2 = -f(r)dt^2 + f^{-1}(r)dr^2 + r^2d\phi^2 , \quad f(r) = 1 - 8G_3M - \frac{r^2}{R_3^2} - \frac{2L_P F(M)}{r} , \quad (2.11)$$

then the redshift factor $f(r)$ has the same form as in the four-dimensional Schwarzschild-de Sitter solution, which does indeed have a black hole horizon. The interpretation of terms, however, is different: the $1/r$ term, which in four dimensions would be associated to the mass, here is due to quantum corrections, while the three-dimensional mass is given by the constant terms. This four-dimensional resemblance of the quantum-corrected geometry is obscure in this setup, but it will become natural within the holographic construction.

3 de Sitter braneworld in AdS₄

We turn now to the approach of braneworld holography. We shall start by reviewing the construction of a de Sitter brane in an AdS₄ bulk.

Its main features can be conveniently understood starting from the metric of the Rindler-AdS₄ spacetime, namely

$$ds^2 = - \left(\frac{\rho^2}{\ell_4^2} - 1 \right) dt_R^2 + \frac{d\rho^2}{\frac{\rho^2}{\ell_4^2} - 1} + \rho^2 (d\vartheta^2 + \sinh^2 \vartheta d\phi^2). \quad (3.1)$$

Orbits of ∂_{t_R} are trajectories of uniform acceleration, and the surface $\rho = \ell_4$ is a non-compact, acceleration horizon, such that AdS₄ is not globally covered in these coordinates. With respect to the canonically normalized time t_R , the horizon has a temperature

$$T_R = \frac{1}{2\pi\ell_4}. \quad (3.2)$$

Let us now rewrite this spacetime after changing spatial coordinates as

$$\frac{\hat{r}^2}{R_3^2} = \frac{\rho^2 \sinh^2 \vartheta}{\rho^2 \cosh^2 \vartheta - \ell_4^2}, \quad \cosh \sigma = \frac{\rho}{\ell_4} \cosh \vartheta, \quad (3.3)$$

and (as a matter of mere convenience, which does not change the patches that are covered)

$$\frac{t}{R_3} = \frac{t_R}{\ell_4}. \quad (3.4)$$

The metric becomes

$$ds^2 = \ell_4^2 d\sigma^2 + \frac{\ell_4^2}{R_3^2} \sinh^2 \sigma \left[- \left(1 - \frac{\hat{r}^2}{R_3^2} \right) dt^2 + \left(1 - \frac{\hat{r}^2}{R_3^2} \right)^{-1} d\hat{r}^2 + \hat{r}^2 d\phi^2 \right]. \quad (3.5)$$

We see that sections of constant σ yield dS₃ in static-patch coordinates with radius given by $\ell_4 \sinh \sigma$. The acceleration horizon in (3.1) is now at $\hat{r} = R_3$, which, as σ varies between 0 and ∞ , traces out the cosmological horizons of the dS₃ sections. That is, the bulk Rindler horizon induces a cosmological horizon on the dS₃ slices of constant σ .

The bulk acceleration horizon is non-compact since it extends all the way to the asymptotic boundary at $\sigma \rightarrow \infty$. It will become a compact horizon if we make our universe compact by introducing a positive-tension brane at

$$\sinh \sigma_b = \frac{R_3}{\ell_4}, \quad (3.6)$$

which excludes all of the region $\sigma > \sigma_b$. If the brane action is purely tensional,

$$I_{\text{brane}} = -\tau \int d^3x \sqrt{-h}, \quad (3.7)$$

then the Israel junction conditions (i.e., the equations of motion of the brane) demand that the tension be

$$\tau = \frac{\cosh \sigma_b}{2\pi G_4 R_3} = \frac{1}{2\pi G_4} \sqrt{\frac{1}{R_3^2} + \frac{1}{\ell_4^2}}. \quad (3.8)$$

For later convenience, instead of the tension τ we will use the associated length scale

$$\ell = \frac{1}{2\pi G_4 \tau}, \quad (3.9)$$

such that $\cosh \sigma_b = R_3/\ell$. Eq. (3.8) becomes

$$\frac{1}{\ell^2} = \frac{1}{R_3^2} + \frac{1}{\ell_4^2}. \quad (3.10)$$

Observe that $\ell < \ell_4$, i.e., for fixed ℓ_4 the brane tension is bounded below in order for $R_3^2 > 0$. Branes with lower tension, $\ell = \ell_4$ and $\ell > \ell_4$, would have Minkowski₃ and AdS₃ worldvolumes, respectively.

The geometry induced on the brane is that of dS₃ with radius R_3 , and the area of the horizon in the bulk is now finite, with a corresponding finite entropy

$$S_{\text{BH}}^{(4)} = \frac{A_H}{4G_4} = \frac{\pi \ell_4^2}{2G_4} (\cosh \sigma_b - 1) = \frac{\pi}{2G_4} \frac{R_3^2 \ell}{R_3 + \ell}. \quad (3.11)$$

An illustration of the resulting spacetime is presented in Fig. 1.

Induced gravity theory

So far we are considering the spacetime and the brane within it in a four-dimensional interpretation. However, in these braneworlds, a mode of the bulk graviton is localized near the brane [21, 22], reproducing a three-dimensional theory of gravity there; in addition, using holography, the remaining bulk graviton modes can be described in terms of a dual three-dimensional CFT. As a result, the entire four-dimensional setup admits a purely three-dimensional description as a classical gravitational theory coupled to a quantum CFT.

The effective theory of gravity on the brane can be regarded as being induced by integrating out the holographic UV degrees of freedom of the dual CFT₃ down to an energy cutoff of $1/\ell$ [23]. The derivation given in [6] for AdS₃ branes is also valid for dS₃ branes, so we skip directly to the result of the integration, namely (see also [9, 24])

$$I_{\text{ind}} = \frac{\ell_4}{8\pi G_4} \int d^3x \sqrt{-h} \left[\frac{4}{\ell_4} \left(\frac{1}{\ell} - \frac{1}{\ell_4} \right) + \tilde{R} + \ell_4^2 \left(\frac{3}{8} \tilde{R}^2 - \tilde{R}_{\mu\nu}^2 \right) + \dots \right], \quad (3.12)$$

where $\tilde{g}_{\mu\nu} = h_{\mu\nu}$ and $\tilde{R}_{\mu\nu}$ are the metric induced on the brane and its Ricci curvature. From here we identify the effective three-dimensional Newton's constant as

$$G_3 \equiv \frac{G_4}{2\ell_4}, \quad (3.13)$$

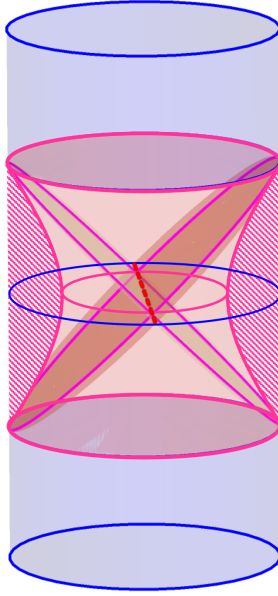


Figure 1: Bulk AdS_4 with a de Sitter₃ brane. The brane is represented as a (magenta) hyperboloid ($\sigma = \sigma_b$ in (3.5)), and gravity is induced on it from integrating out the UV degrees of freedom of the CFT_3 excluded by the brane (dashed magenta region). One performs surgery by gluing two copies of the region $\sigma < \sigma_b$ along the two-sided brane. The brane is following an accelerating trajectory, and the bulk acceleration horizons give rise to cosmological horizons on the induced dS geometry. The red dashed line is the bifurcation surface of the Rindler-AdS horizons. When the brane is introduced, it becomes a compact surface of finite area (3.11).

and the effective three-dimensional cosmological constant,

$$\frac{2}{L_3^2} \equiv \frac{4}{\ell_4} \left(\frac{1}{\ell} - \frac{1}{\ell_4} \right). \quad (3.14)$$

The higher curvature terms in the action are multiplied by higher powers of ℓ_4 , which plays the role of the cutoff length scale of the effective three-dimensional theory. More precisely, in order for the effective three-dimensional theory to be valid we must have

$$\ell_4 \ll L_3, \quad (3.15)$$

which, using (3.10), means that

$$\ell \sim \ell_4 \ll R_3. \quad (3.16)$$

From (3.6) we see that this requires that the brane be close to the boundary, $\sigma_b \gg 1$. We will often regard ℓ/R_3 as the small expansion parameter of the effective theory. Observe that R_3 , which is defined as the physical curvature radius of the brane, is not exactly the same as L_3 due to the higher curvature terms. For small ℓ we find

$$\frac{1}{L_3^2} = \frac{2}{\ell_4^2} \left(\frac{\ell_4}{\ell} - 1 \right) \approx \frac{1}{R_3^2} - \frac{\ell^2}{4R_3^4} + \mathcal{O}(\ell^4/R_3^6). \quad (3.17)$$

The complete three-dimensional effective action I on the brane is the sum of the induced gravity action I_{ind} and the action I_{CFT} of the boundary CFT_3 , determined holographically by the bulk. Using (3.17), to leading order we have

$$I = \frac{1}{16\pi G_3} \int d^3x \sqrt{-h} \left[\tilde{R} - \frac{2}{R_3^2} + \ell^2 \left(\frac{3}{8} \tilde{R}^2 - \tilde{R}_{\mu\nu}^2 \right) + \dots \right] + I_{\text{CFT}}, \quad (3.18)$$

where the ellipsis denotes terms of order $\mathcal{O}(\ell^4)$ and higher. Further, following [6], we normalize the central charge c of the boundary CFT as⁸

$$c = \frac{\ell_4^2}{G_4} \quad \Rightarrow \quad 2cG_3 = \ell_4 \approx \ell \left(1 + \frac{\ell^2}{2R_3^2} + \frac{3}{8} \frac{\ell^4}{R_3^4} + \dots \right). \quad (3.19)$$

Therefore, for fixed c , as $\ell \rightarrow 0$ gravity on the brane becomes weak ($G_3 \rightarrow 0$) such that there is no backreaction due to the CFT. This limit looks singular from the viewpoint of the bulk, since if we want to keep R_3 finite then we must take $\ell_4 \rightarrow 0$. In the naive way of taking this limit we are not only eliminating the backreaction, but removing the CFT_3 altogether by removing the bulk. If instead we take the limit $\ell_4 \rightarrow 0$ while rescaling the bulk metric by a factor ℓ_4^2 , then the brane is pushed to the boundary and gravitational dynamics on the brane is turned off, while still keeping a non-trivial state of the non-backreacting CFT_3 . This limit is described in App. C. Note also that, since the three-dimensional Planck length is $L_P = G_3$ (with $\hbar = 1$), we can write (3.19) as

$$\ell = 2cL_P \left(1 + \mathcal{O} \left(\frac{cL_P}{R_3} \right)^2 \right), \quad (3.20)$$

which will often be useful.

According to the holographic dictionary, the induced metric on the brane solves the semi-classical gravitational equations [6]

$$8\pi G_3 \langle T_{\alpha\beta}^{\text{CFT}} \rangle = \tilde{G}_{\alpha\beta} + \frac{h_{\alpha\beta}}{L_3^2} \quad (3.21)$$

$$+ \ell^2 \left[4\tilde{R}_\alpha^\gamma \tilde{R}_{\beta\gamma} - \frac{9}{4} \tilde{R} \tilde{R}_{\alpha\beta} - \square \tilde{R}_{\alpha\beta} + \frac{1}{4} \nabla_\alpha \nabla_\beta \tilde{R} + \frac{1}{2} h_{\alpha\beta} \left(\frac{13}{8} \tilde{R}^2 - 3\tilde{R}_{\gamma\delta}^2 + \frac{1}{2} \square \tilde{R} \right) \right] + \dots,$$

where the CFT stress-energy tensor sources the effective three-dimensional gravity theory. With quantum backreaction accounted for by $\langle T_{\alpha\beta}^{\text{CFT}} \rangle$, black hole solutions to this model are quantum-corrected black holes [5], such that the classical dynamics of the bulk four-dimensional Einstein theory encodes the quantum dynamics of the dual three-dimensional effective theory.

⁸Here we are working in units where $\hbar = 1$. To recover factors of \hbar , one need only replace $c \rightarrow c\hbar$.

4 Quantum Schwarzschild-de Sitter black hole

Now we introduce one of the main elements in this work: an exact solution to the bulk theory that describes a black hole localized on a dS_3 brane. According to our previous discussion, its dual interpretation is as a black hole solution to the semiclassical Einstein equations (1.6), with the backreaction included exactly, to leading order in the large- c expansion of the quantum CFT_3 . Therefore, we can claim that the solution does describe a quantum black hole in dS_3 .

Our discussion follows a similar analysis presented in [5] for an AdS_3 brane, which led to the quantum BTZ (qBTZ) black hole, but there are some key differences worth highlighting.

4.1 AdS_4 C-metric

We begin with the following solution to Einstein's equation with negative cosmological constant, which is a particular case of the Plebanski-Demianski type-D solutions [25]

$$ds^2 = \frac{\ell^2}{(\ell + xr)^2} \left[-H(r)dt^2 + \frac{dr^2}{H(r)} + r^2 \left(\frac{dx^2}{G(x)} + G(x)d\phi^2 \right) \right], \quad (4.1)$$

where the metric functions $H(r)$ and $G(x)$ are given by

$$H(r) = 1 - \frac{r^2}{R_3^2} - \frac{\mu\ell}{r}, \quad G(x) = 1 - x^2 - \mu x^3. \quad (4.2)$$

Our conventions largely follow [6], however, we have selected $\kappa = +1$ and set $\ell_3^2 = -R_3^2$ such that the brane we introduce is a dS_3 brane of radius R_3 .

Before introducing the brane, these solutions are well known to describe accelerating black holes in AdS_4 [26, 27]. The parameter $\mu > 0$ would be interpreted as related to the mass of the four-dimensional black hole, but we will see that for us the interpretation is different. The parameter $\ell > 0$ is the inverse of the acceleration of the black hole, $A = 1/\ell$, but it is actually the same as the tension length we introduced before: the relation (3.10) also holds when the bulk metric satisfies $R_{AB} = -(3/\ell_4^2)g_{AB}$. The idea is that in our brane construction the tension of the brane provides the acceleration of the black hole that is attached to it, and we take large enough tension that there is an acceleration horizon in the bulk.⁹

The relation between our earlier brane construction and the metric (4.1) becomes apparent if we consider the case when $\mu = 0$ and perform the coordinate transformation

$$\sinh \sigma = \frac{R_3}{\ell_4} \frac{\sqrt{1 - x^2 r^2 / R_3^2}}{|1 + rx/\ell|}, \quad \hat{r} = r \sqrt{\frac{1 - x^2}{1 - x^2 r^2 / R_3^2}}. \quad (4.3)$$

Then the metric (4.1) becomes the same as that of Rindler- AdS , eq. (3.5) (see the left Fig. 2 for a representation of the (r, x) coordinates).

⁹The regimes where the tension and the acceleration are small, without an acceleration horizon, are appropriate for AdS_3 branes, as in [6, 27]. Minkowski branes are obtained in the critical case [26].

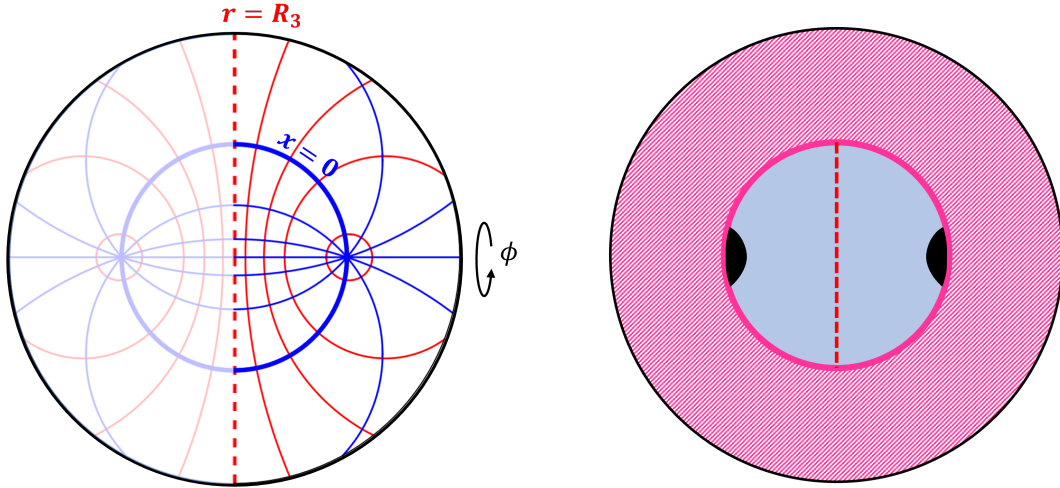


Figure 2: **Left:** AdS₄ C-metric (4.1) with $\mu = 0$, in (r, x) coordinates in a slice at $t = 0$ and constant ϕ . Lines of constant x are blue arcs; lines of constant r are red arcs (full circles for $0 < r < \ell$). The thick blue circle $x = 0$ is where we place the dS₃ brane; its interior is $0 < x \leq 1$, with $x = 1$ the ϕ axis of rotation. The exterior region $x < 0$ is excluded in the braneworld construction. The vertical red dashed line is the horizon at $r = R_3$. Its intersection with the brane yields a dS₃ cosmological horizon. The coordinates only cover half of the disk, with the other half being obtained through analytic continuation. **Right:** construction of black holes on a dS₃ braneworld when $\mu > 0$. The dashed magenta region $x < 0$ is excluded. The black hole horizon and the cosmological horizon are at constant r .

Each zero of the function $G(x)$ corresponds to an axis for the rotation symmetry, with possible conical singularities lying there. Particularly, for a range of values of μ , there will be three distinct zeros to $G(x)$, denoted by $\{x_0, x_1, x_2\}$, with each zero leading to a distinct conical singularity. One of the conical singularities can be removed via the identification,

$$\phi \sim \phi + \frac{4\pi}{|G'(x_i)|}, \quad (4.4)$$

where x_i is one of the select zeros. Once the period of ϕ has been fixed in this way, say at $x = x_1$, then ϕ cannot be readjusted to eliminate the remaining singularities at $x = x_0, x_2$.

Not all of these zeroes of $G(x)$ will be relevant for our discussion, though. We are interested in introducing a brane, which in the case $\mu = 0$ of empty AdS₄ is at (3.6), and in the coordinates of (4.1) corresponds to $x = 0$. A feature of the AdS₄ C-metric that makes it especially suitable for braneworld constructions is that, when $\mu > 0$, the surface $x = 0$ also satisfies the Israel junction conditions for a brane with tension given by (3.9). Thus, the braneworld we seek is obtained by placing such a brane at $x = 0$, and keeping only the

$$x > 0 \quad (4.5)$$

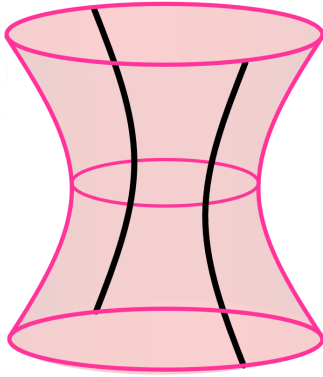


Figure 3: Illustration of the bulk braneworld from the AdS₄ C-metric. The brane is placed at $x = 0$ (magenta hyperboloid surface). The black lines denote $r = 0$ and depict the worldlines of the accelerating black holes described by the C-metric. The AdS interior of the hyperboloid is kept, and the double-sided brane is glued to another copy of it.

portion of the bulk geometry. The metric induced on the brane located at $x = 0$ will be

$$ds^2|_{x=0} = - \left(1 - \frac{\mu\ell}{r} - \frac{r^2}{R_3^2} \right) dt^2 + \left(1 - \frac{\mu\ell}{r} - \frac{r^2}{R_3^2} \right)^{-1} dr^2 + r^2 d\phi^2, \quad (4.6)$$

which is strongly reminiscent of the quantum-backreacted geometry (2.11) that we have encountered before. However, we note two differences. The first one is very significant: the solution (4.6) is exact, so, unlike in (2.11), the term $\propto 1/r$ in the metric coefficients does not need to be treated as a perturbative correction (even though it may be small). The second one is that it is unclear what are the physical parameters of the solution in (4.6): what is the three-dimensional mass M , and how is μ related to the quantum corrections $L_P F(M)$? For this purpose, we must analyze the global properties of the bulk solution.

Bulk regularity

Black holes arise in the AdS₄ C-metric (4.1) when $\mu \neq 0$ (see the right Fig. 2 and Fig. 3). Whether we find a black hole horizon depends on the nature of the roots of the functions $H(r)$ and $G(x)$, where the roots of $H(r)$ correspond to the Killing horizons generated by the time translation Killing vector ∂_t . We desire for positive roots of $H(r)$, if we are to describe physically acceptable horizons. Meanwhile, real roots of $G(x)$ correspond to symmetry axes of the Killing vector ∂_ϕ , and they characterize the geometry of the horizon in the bulk. For instance, a surface of constant r with $0 \leq x \leq x_1$ is a (distorted) half-sphere with disk topology.

Our strategy is to first consider the roots of $G(x)$, where we look for at least one real root. This can be established by specifying a range for the parameter μ [26, 27]. When $\mu > 0$ there will be one positive root, denoted by x_1 , and we restrict the range of x such that $0 \leq x \leq x_1$.

In this way, there is a single conical singularity at $x = x_1$, which may be removed by a proper identification of the period for ϕ , while the remaining conical singularities simply will be absent via the spacetime surgery of introducing a brane at $x = 0$. Following [6], it behooves us to consider the root x_1 as a parameter, while μ is “derived”. That is, from $G(x_1) = 0$ we have

$$\mu = \frac{1 - x_1^2}{x_1^3}, \quad (4.7)$$

with $x_1 \in (0, 1]$. We see μ will monotonically decrease from $+\infty$ to zero, where $\mu = 0$ coincides with $x_1 = 1$. Later we will see that when $\ell \neq 0$ the allowed value of μ will be limited above if we want to have a regular black hole horizon.

The conical singularity at $x = x_1$ is removed via the identification

$$\phi \sim \phi + \Delta\phi, \quad \Delta\phi = \frac{4\pi}{|G'(x_1)|} = \frac{4\pi x_1}{3 - x_1^2}. \quad (4.8)$$

We see for the range of x_1 , the function $G'(x_1) = -\frac{3-x_1^2}{x_1} < 0$, and that $\Delta\phi$ is independent of ℓ and R_3 . Moreover, $\Delta\phi$ grows monotonically from 0 to 2π .

4.2 Black hole on the brane

We now understand that, although the metric (4.6) has the form of asymptotically dS₃ space, the ϕ coordinate is not identified with 2π but rather $\Delta\phi$ (4.8). Then there is a conical deficit angle which signals the effect of a mass. To make it manifest, we change to canonical coordinates $(t, r, \phi) \rightarrow (\bar{t}, \bar{r}, \bar{\phi})$ via

$$t = \eta\bar{t}, \quad r = \frac{\bar{r}}{\eta}, \quad \phi = \eta\bar{\phi}, \quad (4.9)$$

where

$$\eta \equiv \frac{\Delta\phi}{2\pi} = \frac{2x_1}{3 - x_1^2} \quad (4.10)$$

and

$$ds^2|_{x=0} = - \left(\eta^2 - \frac{\mu\ell\eta^3}{\bar{r}} - \frac{\bar{r}^2}{R_3^2} \right) d\bar{t}^2 + \left(\eta^2 - \frac{\mu\ell\eta^3}{\bar{r}} - \frac{\bar{r}^2}{R_3^2} \right)^{-1} d\bar{r}^2 + \bar{r}^2 d\bar{\phi}^2. \quad (4.11)$$

Since now $\bar{\phi} \sim \bar{\phi} + 2\pi$, we can identify η^2 with $1 - 8\mathcal{G}_3 M$ and thus obtain the mass of the solution. Actually, it is convenient to perform the identification as

$$8\mathcal{G}_3 M = 1 - \eta^2 = 1 - \frac{4x_1^2}{(3 - x_1^2)^2}, \quad \mathcal{G}_3 \equiv \frac{\ell_4}{\ell} G_3, \quad (4.12)$$

where we have introduced the renormalized Newton’s constant \mathcal{G}_3 , following [6]. This takes into account the modifications in the definition of the mass due to higher curvature corrections

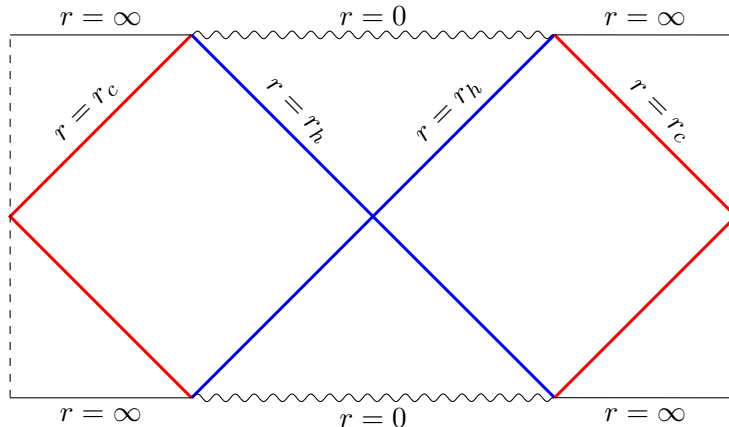


Figure 4: Penrose diagram of a static, neutral quantum black hole in dS_3 .

in the effective gravitational theory, which are then encoded in a ‘renormalized’ Newton’s constant \mathcal{G}_3 [28].¹⁰

By virtue of (4.7) and (4.8), we can respectively replace μ and η with rational polynomials of x_1 . Explicitly, the function $H(\bar{r})$ becomes

$$H(\bar{r}) = \frac{4x_1^2}{(3-x_1^2)^2} - \frac{8\ell}{\bar{r}} \frac{1-x_1^2}{(3-x_1^2)^3} - \frac{\bar{r}^2}{R_3^2}. \quad (4.13)$$

We have related the first term to a mass M and a renormalized Newton’s constant \mathcal{G}_3 ; the additional ℓ/\bar{r} term characterizes quantum corrections to the black hole. It vanishes when $\ell \rightarrow 0$, which is the limit in which the gravitational effects of the CFT are suppressed, and indeed we recover a classical conical defect in dS_3 . For finite ℓ , however, the backreaction leads to a $1/\bar{r}$ (quantum) correction to SdS_3 . Given the relation between x_1 and M in (4.12), we naturally interpret the second term in $H(\bar{r})$ as a function of the mass $F(M)$,

$$F(M) \equiv \frac{8(1-x_1^2)}{(3-x_1^2)^3}. \quad (4.14)$$

Altogether then, we recast the metric on the brane (4.11) as

$$ds^2|_{x=0} = -H(\bar{r})d\bar{t}^2 + H^{-1}(\bar{r})d\bar{r}^2 + \bar{r}^2d\bar{\phi}^2, \quad H(\bar{r}) = 1 - 8\mathcal{G}_3M - \frac{\ell F(M)}{\bar{r}} - \frac{\bar{r}^2}{R_3^2}. \quad (4.15)$$

4.3 Nariai Limit

When $\mu \neq 0$, the metric function $H(r)$ (4.2) takes the same form as the blackening factor of a four-dimensional Schwarzschild-de Sitter black hole [29]. Thus, we have a (smaller) black

¹⁰We point out the relation $\mathcal{G}_3 \equiv \frac{\ell^4}{\ell} G_3$ is assumed to hold for all orders in ℓ and may be interpreted as a resummation of higher curvature corrections to the mass at all orders in ℓ .

hole horizon $r = r_h$ aside from the cosmological horizon $r = r_c$, each as a positive root of $H(r)$, with $r_h < r_c$. Consequently, setting $H(r_h) = H(r_c) = 0$, we may express the de Sitter radius R_3 and $\mu\ell$ entirely in terms of horizon radii r_h and r_c ,

$$R_3^2 = \frac{r_c^3 - r_h^3}{r_c - r_h} = r_c^2 + r_h^2 + r_c r_h, \quad \mu\ell = \frac{r_h r_c^3 - r_h^3 r_c}{r_c^3 - r_h^3} = \frac{r_c r_h (r_c + r_h)}{r_c^2 + r_h^2 + r_h r_c}. \quad (4.16)$$

Note the form factor $H(r)$ factorizes in terms of r_c and r_h

$$H(r) = \frac{1}{R_3^2 r} (r R_3^2 - r^3 - \mu\ell R_3^2) = \frac{1}{R_3^2 r} (r - r_h)(r_c - r)(r + r_c + r_h). \quad (4.17)$$

In the limit $r_h \rightarrow 0$, we recover the pure dS₃ slicing (coinciding with $\mu = 0$). Moreover, note that the curvature singularity at $r = 0$ is hidden behind the induced black hole horizon (see the Penrose diagram in Fig. 4).

As $\mu\ell$ increases, the size of the black hole will increase until eventually it saturates the size of the cosmological horizon, the well-known Nariai limit [11, 12] of the SdS black hole, where $r_c = r_h \equiv r_N$, the Nariai radius. The resulting mass of the black hole forms an upper bound on $(\mu\ell)$, denoted $(\mu\ell)_N$, to avoid a naked singularity. By setting $H(r_N) = H'(r_N) = 0$, we find the Nariai radius r_N and maximum size of $(\mu\ell)_N$

$$r_N = \frac{1}{\sqrt{3}} R_3, \quad (\mu\ell)_N = \frac{2}{3} r_N = \frac{2}{3\sqrt{3}} R_3. \quad (4.18)$$

Therefore, when $\ell \neq 0$ the Nariai limit places an upper bound on μ .

Note that the relation (4.16) may be inverted to find closed form expressions of $r_{h,c}$ in terms of μ and r_N (see, *e.g.*, [30, 31])

$$r_h = r_N (\cos \omega - \sqrt{3} \sin \omega), \quad r_c = r_N (\cos \omega + \sqrt{3} \sin \omega), \quad \text{with } \omega \equiv \frac{1}{3} \arccos \left(\frac{\mu}{\mu_N} \right). \quad (4.19)$$

This relation will prove useful for plotting, see Fig. 5. Moreover, we see that the horizon radii are proportional to r_N and hence to ℓ , which is much larger than the Planck radius when $R_3 \gg \ell$, cf. (3.19) (see also below).

Thus, in the limit $\mu\ell \rightarrow (\mu\ell)_N$, the function $H(r)$ will have a double root at r_N . The region between these two roots describes the finite Nariai black hole solution.¹¹ However, we cannot use coordinates (t, r) to describe the Nariai metric since $H(r)$ vanishes in the region between the two horizons. To find the correct geometry, we follow [34] and introduce dimensionful coordinates (τ, ρ) and a real, positive parameter β

$$\tau = \epsilon t, \quad \rho = \frac{r - r_h}{\epsilon}, \quad \beta = \frac{r_c - r_h}{\epsilon}, \quad (4.20)$$

where ϵ is a dimensionful parameter quantifying the distance between radii r_c and r_h . Taking the limit $r_h, r_c \rightarrow r_N$ and $\epsilon \rightarrow 0$, one finds the Nariai limit of the geometry (4.1),

$$ds^2 = \frac{\ell^2}{(\ell + x r_N)^2} \left[-\frac{\rho(\beta - \rho)}{r_N^2} d\tau^2 + r_N^2 \frac{d\rho^2}{\rho(\beta - \rho)} + r_N^2 \left(\frac{dx^2}{G(x)} + G(x) d\phi^2 \right) \right]. \quad (4.21)$$

¹¹See [32, 33] for previous studies of the Nariai-like limit of the C-metric.

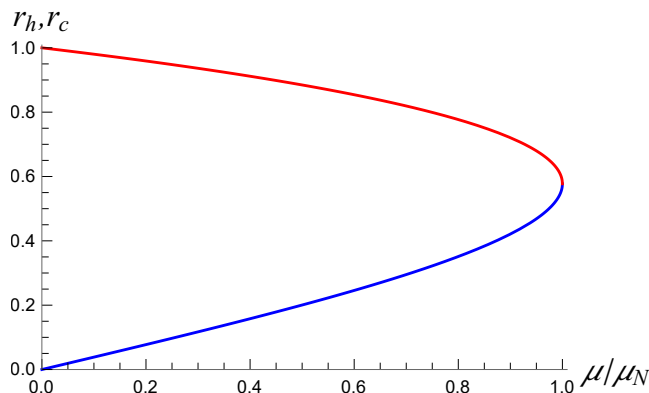


Figure 5: Plot of the horizon radii r_h (blue) and r_c (red) as a function of μ/μ_N . The black hole horizon becomes larger as μ grows, while the cosmological horizon shrinks.

In these coordinates, the black hole horizon lives at $\rho = 0$ while the cosmological horizon is at $\rho = \beta$. Further, performing the coordinate transformation

$$\tilde{\tau} = \frac{\beta}{2r_N} \tau, \quad \tilde{\rho} = \frac{2r_N}{\beta} (\rho - \beta/2) \quad (4.22)$$

brings the line element (4.21) to the form

$$ds^2 = \frac{\ell^2}{(\ell + xr_N)^2} \left[- \left(1 - \frac{\tilde{\rho}^2}{r_N^2} \right) d\tilde{\tau}^2 + \left(1 - \frac{\tilde{\rho}^2}{r_N^2} \right)^{-1} d\tilde{\rho}^2 + r_N^2 \left(\frac{dx^2}{G(x)} + G(x)d\phi^2 \right) \right]. \quad (4.23)$$

The $(\tilde{\tau}, \tilde{\rho})$ geometry is two-dimensional de Sitter space with length scale r_N , while the (x, ϕ) sector describes (distorted) half-spheres of curvature radius r_N .

4.4 Solution parameters and validity range: 4D and 3D views

Let us pause for a moment to compare the two different ways of viewing the solution and the three parameters that characterize it. From the perspective of the bulk, these are naturally taken to be

$$\ell_4, \quad \ell, \quad \mu \quad (4.24)$$

corresponding to the bulk cosmological radius, the brane tension, and the bulk black hole parameter. In the three-dimensional interpretation it is more natural to take them to be

$$R_3, \quad cG_3, \quad \mathcal{G}_3 M \quad (4.25)$$

namely, the dS_3 radius, the gravitational backreaction parameter, and the three-dimensional black hole mass. For convenience, we summarize here the relations between the two sets as

$$\ell_4 = 2cG_3, \quad \text{or} \quad \ell = 2cG_3 \left(1 + \mathcal{O}(cG_3/R_3)^2 \right), \quad (4.26)$$

$$\frac{1}{\ell^2} - \frac{1}{\ell_4^2} = \frac{1}{R_3^2}, \quad (4.27)$$

and

$$\mu = 1 - \frac{1 - x_1^2}{x_1^3}, \quad 8\mathcal{G}_3 M = 1 - \frac{4x_1^2}{(3 - x_1^2)^2}. \quad (4.28)$$

The first relation is also given expanded for small backreaction $cG_3/R_3 \ll 1$. The last one is in parametric form. The ‘renormalized’ Newton’s constant is

$$\mathcal{G}_3 = \frac{G_4}{2\ell} = \frac{\ell_4}{\ell} G_3 = G_3 + \mathcal{O}(cG_3/R_3)^2. \quad (4.29)$$

Bear in mind, though, that the Newton constants, in three or four dimensions, do not enter as additional independent parameters of the solutions.

As we mentioned above, the effective theory expansion (3.12) indicates that the cutoff length scale of the three-dimensional effective theory is ℓ_4 , i.e., cL_P . When there is a large number of quantum fields, $c \gg 1$, this length scale is much larger than the quantum gravity scale L_P . In other words, the cutoff energy is much lower than the naive one, a phenomenon already noted in [5] in the context of braneworld holography, and which is well known in more generality [35]. The black holes that we have constructed have a size $\propto cL_P$, and their length scales never acquire values much larger than cL_P , e.g., $F(M)$ is never very large. Thus, in principle they may be subject to threshold effects of the effective theory.

On the other hand, from the bulk viewpoint there is no problem in considering black holes with sizes smaller than ℓ_4 – only that, since they involve sub-AdS scales, they are harder to understand from the dual CFT viewpoint. Our viewpoint in this article is that any AdS space can be viewed as a definition of a cutoff CFT. This does not guarantee the existence of its ultraviolet completion, but as long as the only degrees of freedom that are added at the cutoff scale are the KK graviton modes, then our black holes are accurately described by the bulk solution.¹² The classical bulk description is reliable as long as the black holes are larger than the four-dimensional Planck length, which is the case when $c \gg 1$.

With these caveats in mind, we can regard our black holes as valid solutions of the quantum backreaction problem.

4.5 Backreaction and quantum black holes

With the metric (4.15) in hand, we can, in principle, systematically compute the renormalized stress-tensor to all orders in ℓ using the right-hand side of the equations of motion (3.21). To do this, we use the expansion of length scales (3.17) and perturbatively expand $\langle T_{\alpha\beta}^{\text{CFT}} \rangle$ in powers of ℓ^2 , such that

$$\langle T_{\alpha\beta}^{\text{CFT}} \rangle = \langle T_{\alpha\beta}^{\text{CFT}} \rangle_0 + \ell^2 \langle T_{\alpha\beta}^{\text{CFT}} \rangle_2 + \dots. \quad (4.30)$$

¹²See [5] for a more extensive discussion.

The analysis can be piggy-backed on the one in AdS₃ via $\ell_3 \rightarrow iR_3$, so we refer to [6] for details. The result is

$$\langle T_{\beta}^{\alpha} \rangle_0 = \frac{c}{8\pi} \frac{F(M)}{\bar{r}^3} \text{diag}(1, 1, -2), \quad (4.31)$$

where we have substituted $\ell = 2cG_3$. This clearly has zero trace. With a little more work, the stress tensor at $\mathcal{O}(\ell^2)$ is

$$\begin{aligned} \langle T_{\beta}^{\alpha} \rangle_2 = & \frac{\ell}{16\pi G_3} \frac{F(M)}{\bar{r}^3} \left(-\frac{1}{2R_3^2} \text{diag}(1, -11, 10) - \frac{24\mathcal{G}_3 M}{\bar{r}^2} \text{diag}(3, 1, -4) \right. \\ & \left. + \frac{\ell F(M)}{2\bar{r}^3} \text{diag}(-29, -17, 43) \right). \end{aligned} \quad (4.32)$$

This $\mathcal{O}(\ell^2)$ contribution $\langle T_{\beta}^{\alpha} \rangle_2$ has a non-zero trace, thus breaking the conformal symmetry due to the cutoff ℓ .

We could in principle continue this calculation and derive higher-order contributions to $\langle T_{\alpha\beta}^{\text{CFT}} \rangle$, simply by expanding the induced action to higher orders in ℓ . This is a distinct technical advantage over the more standard approach carried out in Sec. 2. Comparing to [6], we see this is related to the backreaction on a quantum BTZ black hole background via the Wick rotation $\ell_3 \rightarrow iR_3$.

In the limit $\ell \rightarrow 0$, the metric (4.15) becomes the standard (no black hole) Schwarzschild-de Sitter solution in three dimensions. Thus, given the above discussion, for $\ell > 0$, it is natural to interpret (4.15) as a quantum black hole in three-dimensional de Sitter space, namely, the *quantum Schwarzschild-de Sitter* solution (qSdS).

There are three special limits of the qSdS solution to consider. One is the Nariai limit, which we will describe in more detail momentarily. To describe the other two limits, note that μ and ℓ are technically independent parameters. This leads to the first important limit of the qSdS solution. Specifically, from the definition for μ (4.7), recall $\mu = 0$ implies $x_1 = 1$. Equivalently, via (4.12) and (4.14), $x_1 = 1$ corresponds with $M = 0$ and $F(M) = 0$ on the brane, respectively. Hence $\mu = 0$ removes the $O(1/r)$ term from the blackening factor along with the black hole horizon. Therefore, $\mu = 0$ (or $x_1 = 1$) yields the three-dimensional *quantum de Sitter* spacetime (qdS₃), accounting for the backreaction of quantum fields outside of the cosmological horizon when $\ell \neq 0$. Lastly, in the infinite R_3 limit, the $O(r^2/R_3^2)$ in the blackening factor is negligible, leading to a *quantum Schwarzschild* black hole. In the next section we will be more careful with this limit, where we see small qSdS black holes (with $R_3 \gg r_h$) behave thermodynamically like a flat Schwarzschild solution.

Comparing $\langle T_{\beta}^{\alpha} \rangle$

The renormalized stress-energy tensor for the non-backreacted conformal fields turns out to have the form of (1.4), whether we obtain it using holography or solving the quantum theory of a free conformal scalar in a conical geometry. Even though the two methods of calculation are completely different, they only differ in the mass dependence of the function $F(M)$, which

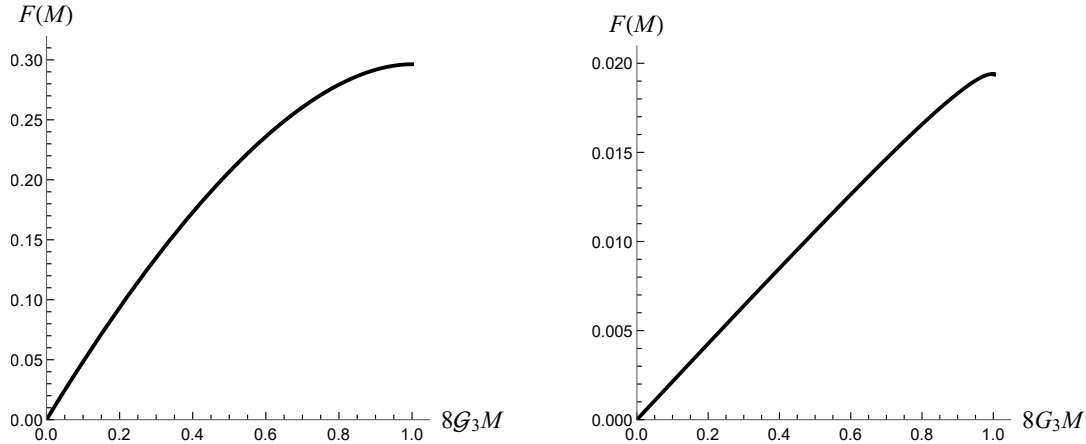


Figure 6: **Left:** Form factor $F(M)$ computed holographically. When backreaction is present, the upper bound in the mass, set by the Nariai limit, is lower. **Right:** $F(M)$ found from renormalized stress tensor of a single conformal scalar in conical dS_3 . For comparison, the holographic result must be multiplied by the central charge $c \gg 1$.

is actually expected since each approach has different field content – and actually, the shapes of $F(M)$ do not differ strongly, as we can see in Fig. 6.

We can understand that in both cases $\langle T_{\beta}^{\alpha} \rangle \propto 1/r^3$. This behavior is natural given the scale invariance of the system, but it is not automatically dictated by it, since in a dS_3 geometry the stress tensor could, in addition to depending on G_3M , also depend on R_3/r . However, as shown in [7], the stress tensor for a conformal field in conical dS_3 can be obtained, by a Weyl transformation, from the stress tensor in conical Minkowski spacetime, and in the latter case, conformal symmetry does dictate the $1/r^3$ dependence. Observe that this radial dependence of the stress tensor gives rise to the $1/r$ corrections in the metric.

The stress tensors also have the same tensorial structure $\text{diag}(1, 1, -2)$. Conformal invariance requires tracelessness, but this would still allow for another independent tensor structure, e.g., $\text{diag}(-2, 1, 1)$ (which would correspond to a thermal state). The agreement between our holographic and free field calculations simply reflects that in both cases the fields have transparent boundary conditions. For free fields, this was an explicit choice we made in (2.2), while these conditions are naturally selected in the holographic setup, since bulk fluctuations (dual to conformal field excitations) can freely travel in the bulk.

Nariai limit of the qSdS solution

A chief difference between the quantum BTZ [6] and qSdS solutions is that the latter has both a cosmological and black hole horizon. This is also in contrast to the classical three-dimensional SdS solution, which only has a cosmological horizon. Further, as we reviewed in the bulk geometry, there is a Nariai limit (4.18) for which the black hole and cosmological horizons coincide, leading to the Nariai geometry of the AdS_4 C-metric (4.23). This geometry

is also imprinted on the brane, such that the qSdS system has a well-defined Nariai limit. Following the same steps leading to (4.23), we can likewise find the Nariai limit of the quantum SdS black hole (4.15). Specifically, one finds

$$ds^2|_{x=0} = - \left(1 - \frac{\tilde{\rho}^2}{\tilde{r}_N^2}\right) d\tilde{\tau}^2 + \left(1 - \frac{\tilde{\rho}^2}{\tilde{r}_N^2}\right)^{-1} d\tilde{\rho}^2 + \tilde{r}_N^2 d\tilde{\phi}^2, \quad (4.33)$$

where $\tilde{\tau} = \frac{\tilde{\beta}}{2\tilde{r}_N}\tau$ and $\tilde{\rho} \rightarrow \eta\tilde{\rho}$. The geometry describes $dS_2 \times S^1$, where the curvature radii of dS_2 and the circle S^1 are \tilde{r}_N .

As is well known for the classical four-dimensional SdS black hole, the Nariai limit of the qSdS solution yields an upper bound on the mass, denoted M_N . The mass can be determined as follows. First invert the definition of μ (4.7) to express $x_1(\mu)$. Upon substituting $x_1(\mu)$ into the definition of the mass (4.12), we have $M(\mu)$. The Nariai mass is then $M_N = M(\mu_N)$, where $\mu_N = \frac{2}{3\sqrt{3}}(R_3/\ell)$. While the resulting expression is complicated, it is a monotonically increasing function which is consistent with the range (1.8), *i.e.*, $M_N < 1/(8\mathcal{G}_3)$, which comes from demanding that the conical deficit is less than 2π . Precisely, for $R_3/\ell \rightarrow \infty$ (with $R_3 > \ell$), then the function $M_N(R_3/\ell)$ is approximated by,

$$8\mathcal{G}_3 M_N \approx 1 - \frac{2^{4/3}}{3} \frac{1}{(R_3/\ell)^{2/3}} + \dots, \quad (4.34)$$

where the ellipsis corresponds to higher inverse powers of (R_3/ℓ) . Moreover, in the limit $R_3 \approx \ell$, we find a non-zero lower bound on the Nariai mass,

$$8\mathcal{G}_3 M_N \approx \frac{11}{27} + \frac{160}{729}(R_3/\ell - 1) + \dots. \quad (4.35)$$

Combined, the Nariai mass lies in the range

$$\frac{11}{27} < 8\mathcal{G}_3 M_N < 1. \quad (4.36)$$

Thus, the Nariai bound $M < M_N$ is more stringent than the conical defect bound $M < 1/8\mathcal{G}_3$ for finite R_3/ℓ , coinciding only when $R_3/\ell \rightarrow \infty$. Consequently, due to gravitational quantum backreaction there is a limit on the amount of mass that one can put in dS_3 , which does not saturate the maximum conical deficit angle. Since this is only due to the existence of a Nariai limit on the black hole solutions, it is likely to be present for non-holographic quantum black holes. However, the specific value of the mass bound depends on the details of the quantum theory.

Lastly, the Nariai solution places a bound on the quantum backreaction due to the CFT for which a quantum black hole in dS_3 exists. Particularly, for non-vanishing backreaction there exists a maximum value of $F(M)$ (or equivalently μ) via (4.18), and thus a maximum value of $\Delta\phi$. If the deficit angle grows too large, then the backreaction creates a black hole too large to fit inside dS_3 , such that the mass exceeds the Nariai bound. For such deficits, the quantum SdS solution no longer exists, but rather a naked conical defect spacetime with an *unexcited* CFT. This means that in Fig. 6 the curve for $F(M)$ only extends in mass up to the Nariai bound, which depends on the backreaction parameter.

5 Thermodynamics of the quantum SdS black hole

Above we found a black hole solution on the brane $x = 0$, which, from the brane perspective, is naturally interpreted as a quantum dS₃ black hole, whose black hole horizon is generated due to the presence of a backreacting CFT. The form of the metric is reminiscent of the classical four-dimensional SdS solution, owing to its origin as a black hole in a classical four-dimensional bulk.

Here we further our analysis of the qSdS solution by studying its horizon thermodynamics. In a certain respect, the qSdS thermodynamics is richer than the thermodynamics of the quantum BTZ solution since the qSdS solution has both a cosmological and black hole horizon. Consequently, we will find an entropy and temperature associated with each horizon, and explore the interplay between each system. The analysis below not only provides an important case study of the thermodynamics of quantum de Sitter black holes, it lends another non-trivial consistency check of braneworld holography.

Mass

As discussed above, the system has three parameters, and once we fix a scale, there only remain two dimensionless parameters to characterize it. It is natural to take them as measuring the black hole size and the backreaction length scale ℓ in units of the dS₃ radius. Thus, we follow [6, 27] and introduce

$$z \equiv \frac{R_3}{r_+ x_1}, \quad (5.1)$$

and

$$\nu \equiv \frac{\ell}{R_3}, \quad (5.2)$$

as convenient dimensionless parameters. The latter obviously measures the strength of backreaction for fixed R_3 , while z , which is real and non-negative, is conveniently defined in terms of $r = r_+$, a positive real root of $H(r)$ for a horizon, and x_1 , which characterizes the pole of the horizon along the bulk symmetry axis. We emphasize r_+ represents either the black hole horizon r_h or the cosmological horizon r_c . Correspondingly, we often write $z_{h,c} = \frac{R_3}{r_{h,c} x_1}$.

Two limits worth noting are: the limit of empty quantum de Sitter, which corresponds to $\mu = 0$, i.e., $x_1 = 1$ and $r_+ = R_3$, so we recover it for $z = 1$; and the zero-backreaction limit, $\ell \rightarrow 0$, in which there is no black hole, i.e., $r_h = 0$, and $z_h \rightarrow +\infty$.

We can now express x_1 , μ , and r_+ solely in terms of parameters (5.1) and (5.2). Solving $H(r_+) = 0$ for x_1^2 yields

$$x_1^2 = \frac{1}{z^2} \frac{1 + \nu z^3}{1 + \nu z}. \quad (5.3)$$

Rearranging z (5.1), squaring and substituting in x_1^2 (5.3) leads to

$$r_+^2 = R_3^2 \frac{1 + \nu z}{1 + \nu z^3}. \quad (5.4)$$

Similarly, from $\mu = (1 - x_1^2)/x_1^3$, we find

$$\mu x_1 = \frac{z^2 - 1}{1 + \nu z^3} . \quad (5.5)$$

Notice the quantities (5.3), (5.4), and (5.5) are the Wick rotated counterparts of the qBTZ solution [6].¹³ Lastly, in terms of ν and z , the relation between the bare Newton's constants G_4 and G_3 is

$$G_4 = 2\ell_4 G_3 = \frac{2G_3 \ell}{\sqrt{1 - \nu^2}} , \quad (5.6)$$

while the renormalized Newton's constant (4.12) is

$$\mathcal{G}_3 = \frac{\ell_4}{\ell} G_3 = \frac{G_3}{\sqrt{1 - \nu^2}} . \quad (5.7)$$

Putting together the relations (5.3), (5.4), (5.5), the mass M (4.12) is recast as

$$M = \frac{1}{8G_3} \sqrt{1 - \nu^2} \frac{(z^2 - 1)(9z^2 - 1 + 8\nu z^3)}{(3z^2 - 1 + 2\nu z^3)^2} . \quad (5.8)$$

Further, the function $F(M)$ (4.14) in terms of z and ν is

$$F(M) = \frac{8z^4(z^2 - 1)(1 + \nu z)^2}{(3z^2 - 1 + 2\nu z^3)^3} . \quad (5.9)$$

In the quantum de Sitter limit, where $z = 1$, we have $M = 0$ and $F(M) = 0$, as expected. It is also worth pointing out that the mass M will vanish at large z ,

$$\lim_{z \rightarrow \infty} M \approx \frac{1}{4\mathcal{G}_3 \nu z} + \mathcal{O}(1/z^2) . \quad (5.10)$$

For fixed $x_1 \neq 1$ and for $z = z_h$, it is natural to think of the large z_h limit as a *small* quantum Schwarzschild black hole, where $R_3 \gg r_h x_1$. We will revisit this special case momentarily.

There are two additional limits of the mass (5.8) worth emphasizing. First, in the limit of vanishing backreaction, $\nu \rightarrow 0$, the mass M simplifies to

$$\lim_{\nu \rightarrow 0} M = \frac{1}{8G_3} \frac{(z^2 - 1)(9z^2 - 1)}{(3z^2 - 1)^2} . \quad (5.11)$$

We will utilize this relation below shortly. Second, recall that the black hole has a Nariai limit (4.33), where $(\mu\ell)$ attains a maximum (4.18), such that

$$\mu_N = \frac{2}{3\sqrt{3}} \frac{1}{\nu} . \quad (5.12)$$

Since in the Nariai limit, $r_h = r_c = r_N$, we can introduce a z_N ,

$$z_N = \frac{R_3}{r_N x_1^N} = \frac{\sqrt{3}}{x_1^N} , \quad (5.13)$$

¹³Specifically, with $\ell_3^2 \rightarrow -R_3^2$, we have $z^2 \rightarrow -z^2$, $\nu^2 \rightarrow -\nu^2$ and $\nu z \rightarrow \nu z$.

where x_1^N is the particular value of x_1 in the Nariai limit, found by solving $\mu_N = (1 - x_1^2)/x_1^3$ for x_1 . For arbitrary ν , there will generally be two complex solutions of x_1 and one real solution, which for small ν takes the form

$$x_1^N = \sqrt{3} \left(\frac{\nu}{2}\right)^{1/3} - \frac{\sqrt{3}}{2}\nu + \mathcal{O}(\nu^{5/3}), \quad (5.14)$$

and vanishes in the limit $\nu \rightarrow 0$. The mass of the Nariai solution M_N is therefore defined by $M_N \equiv M|_{z=z_N}$. Further, in the limit $\nu \rightarrow 0$, we find $M_N = \frac{1}{8G_3}$, which is equivalent to the large- z limit of (5.11).

Temperature

From the brane perspective, the black hole and cosmological horizons will appear to emit radiation at the Hawking and Gibbons-Hawking temperatures T_h, T_c , respectively,

$$T_{h,c} = \frac{\kappa_{h,c}}{2\pi}, \quad (5.15)$$

where $\kappa_{h,c}$ are the associated surface gravities, defined by $\xi^\mu \nabla_\mu \xi^\nu = \kappa \xi^\nu$, where ξ is the time-translation Killing vector, $\xi = \partial_{\bar{t}}$. Thus, in terms of ν and z ,

$$T_{h,c} = \frac{|H'(\bar{r}_+)|}{4\pi} = \frac{1}{4\pi} \left| \frac{\mu\ell\eta^3}{\bar{r}_+^2} - \frac{2\bar{r}_+}{R_3^2} \right| = \frac{z}{2\pi R_3} \frac{|2 + 3\nu z - \nu z^3|}{3z^2 - 1 + 2\nu z^3}. \quad (5.16)$$

More explicitly, the temperatures T_h and T_c are given by

$$T_h = -\frac{z_h}{2\pi R_3} \frac{2 + 3\nu z_h - \nu z_h^3}{3z_h^2 - 1 + 2\nu z_h^3}, \quad T_c = \frac{z_c}{2\pi R_3} \frac{2 + 3\nu z_c - \nu z_c^3}{3z_c^2 - 1 + 2\nu z_c^3}. \quad (5.17)$$

In the limit $\nu \rightarrow 0$, the black hole temperature vanishes, since z_h blows up in that case. The cosmological horizon temperature reduce in that limit to

$$\lim_{\nu \rightarrow 0} T_c = \frac{1}{\pi R_3} \frac{z_c}{3z_c^2 - 1}. \quad (5.18)$$

Further, for non-zero $\nu \neq 0$, we see the cosmological horizon of the quantum de Sitter solution is simply the Gibbons-Hawking temperature, $T_c|_{z=1} = 1/(2\pi R_3)$, *i.e.*, the backreaction does not alter the temperature in qdS₃.

Since $r_h < r_c$, we have $z_c < z_h$, and, consequently, the black hole horizon is hotter than the cosmological horizon $T_h > T_c$. Thus, as usual for Schwarzschild-de Sitter spacetimes, the black hole and cosmological horizons are not in thermal equilibrium. Only in the Nariai limit do the temperatures agree with each other, where the system is in thermal equilibrium.

The Nariai limit, however, is subtle because the surface gravities associated with the Killing vector $\partial_{\bar{t}}$ vanish in this limit. To see this, note that the surface gravities κ_h and κ_c for the normalization $\xi = \partial_{\bar{t}}$ are

$$\kappa_h = \frac{1}{2} H'(\bar{r}_h) = \frac{1}{2\bar{r}_h r_N^2} (\bar{r}_N^2 - \bar{r}_h^2), \quad \kappa_c = -\frac{1}{2} H'(\bar{r}_c) = -\frac{1}{2\bar{r}_c r_N^2} (\bar{r}_N^2 - \bar{r}_c^2), \quad (5.19)$$

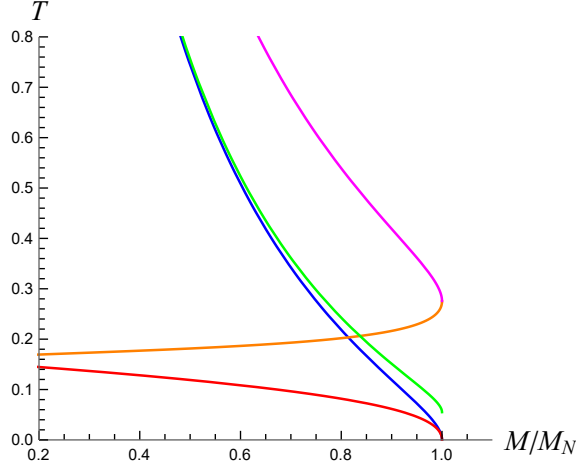


Figure 7: Plot of the temperature as a function of mass M for $\nu = 1/3$. The blue and red curves correspond to temperatures T_h and T_c , respectively, while the magenta and orange curves correspond to \bar{T}_h and \bar{T}_c , respectively. The green curve represents the temperature of the Schwarzschild limit, where $R_3 \gg r_h$, coinciding with T_h for small mass qSdS black holes.

which vanish in the limit $\bar{r}_{h,c} \rightarrow \bar{r}_N$. Consequently, $T_{h,c} \rightarrow 0$ as $\bar{r}_{h,c} \rightarrow \bar{r}_N$. If, however, the Killing vector is normalized as $\xi^2 = -1$ at the radius \bar{r}_0 where the blackening factor $H(\bar{r})$ obtains a maximum, then the surface gravities are non-vanishing in the Nariai limit [36]. Specifically,

$$H'(\bar{r}_0) = 0 \quad \rightarrow \quad \bar{r}_0^3 = \frac{1}{2} \ell F(M) R_3^2 = \frac{\bar{r}_+}{2} (3\bar{r}_N^2 - \bar{r}_+^2). \quad (5.20)$$

Then,

$$H(\bar{r}_0) = 1 - 8\mathcal{G}_3 M - \frac{\ell F(M)}{\bar{r}_0} - \frac{\bar{r}_0^2}{R_3^2} = \frac{1}{r_N^2} (\bar{r}_N^2 - \bar{r}_0^2). \quad (5.21)$$

The new temperature \bar{T} , which was introduced in [36], is

$$\bar{T} = \frac{T}{\sqrt{H(\bar{r}_0)}}. \quad (5.22)$$

In terms of the horizon radii $\bar{r}_{h,c}$, we have

$$\bar{T}_{h,c} = \mp \frac{1}{4\pi r_N \bar{r}_{h,c}} \frac{\bar{r}_N^2 - \bar{r}_h^2}{\sqrt{\bar{r}_N^2 - \left(\frac{\bar{r}_{h,c}}{2} (3\bar{r}_N^2 - \bar{r}_{h,c}^2)\right)^{2/3}}}, \quad (5.23)$$

where the minus sign corresponds to the black hole temperature, and the plus sign to the cosmological horizon temperature. Carefully taking the limit $\bar{r}_N \approx \bar{r}_{h,c}$, the temperature $\bar{T}_{h,c}$ of both horizons approaches the Nariai temperature $T_N = 1/(2\pi r_N)$ (see App. B in [14]). The

expression for \bar{T} in terms of z is cumbersome, however, in the small ν limit we have

$$\bar{T}|_{\nu \approx 0} = \frac{1}{2\pi R_3} \left[1 + \frac{3}{2} \left(\frac{z(z^2 - 1)\nu}{2} \right)^{2/3} + \mathcal{O}(\nu) + \dots \right], \quad (5.24)$$

while for $z = 1$, $\bar{T} = 1/(2\pi R_3)$, the Gibbons-Hawking temperature of dS₃, as expected.

In Fig. 7 we plot the temperatures T_c , T_h , and \bar{T} as a function of mass M . The behavior of the temperatures are essentially identical to that of classical four-dimensional Schwarzschild-de Sitter black holes (see, for instance Fig. 2 of [31]). In particular, notice for small mass M black holes, the black hole temperature diverges, such that it may be approximated by the temperature of a (quantum) Schwarzschild black hole,

$$T_{\text{Schwarz}} = \frac{1}{2\pi R_3} \frac{\nu z_h^2 (z_h^2 - 1)}{(-1 + 3z_h^2 + 2\nu z_h^3)}, \quad (5.25)$$

which follows from dropping the second term in the first equality of (5.16), using the approximation $R_3 \gg r_h$. As seen in Fig. 7, the black hole temperature T_h of the qSdS solution approaches the Schwarzschild temperature (5.25) at small mass. Collectively, our observations indicate the three-dimensional quantum Schwarzschild-de Sitter system, at least thermodynamically, behaves like a four-dimensional classical SdS spacetime, reflecting the holographic character of our setup. We will see additional evidence of this below.

Entropy

For $\mu \neq 0$, the bulk will have two horizons, r_h and r_c . The entropy $S_{\text{BH}}^{(4)}(r_+)$ of either bulk horizon is given by the (four-dimensional) Bekenstein-Hawking entropy-area relation

$$\begin{aligned} S_{\text{BH}}^{(4)} &= \frac{\text{Area}(r_+)}{4G_4} = \frac{2}{4G_4} \int_0^{2\pi\eta} d\phi \int_0^{x_1} dx r_+^2 \frac{\ell^2}{(\ell + x r_+)^2} \\ &= \frac{\pi R_3}{G_3} \frac{z\sqrt{1-\nu^2}}{3z^2 - 1 + 2\nu z^3}, \end{aligned} \quad (5.26)$$

where in the final line we used that G_4 is related to G_3 via (5.6). Again, here it is understood z represents either z_h or z_c , such that the entropy is localized around each horizon.

From the brane perspective, this quantity is interpreted as the sum of the gravitational entropy plus the entanglement entropy due to the backreacting CFT, *i.e.*, the three-dimensional generalized entropy $S_{\text{gen}}^{(3)}$,

$$S_{\text{BH}}^{(4)} = S_{\text{gen}}^{(3)}. \quad (5.27)$$

Note that $S_{\text{gen}}^{(3)}$ is valid to all orders in ν since it is defined as a bulk magnitude, which is *exact*, up to bulk quantum corrections. In the limit $z = 1$, we have the generalized entropy of the quantum de Sitter solution,

$$S_{\text{gen}}^{(3)}|_{z=1} = \frac{2\pi R_3}{4G_3} \frac{\sqrt{1-\nu^2}}{1+\nu}, \quad (5.28)$$

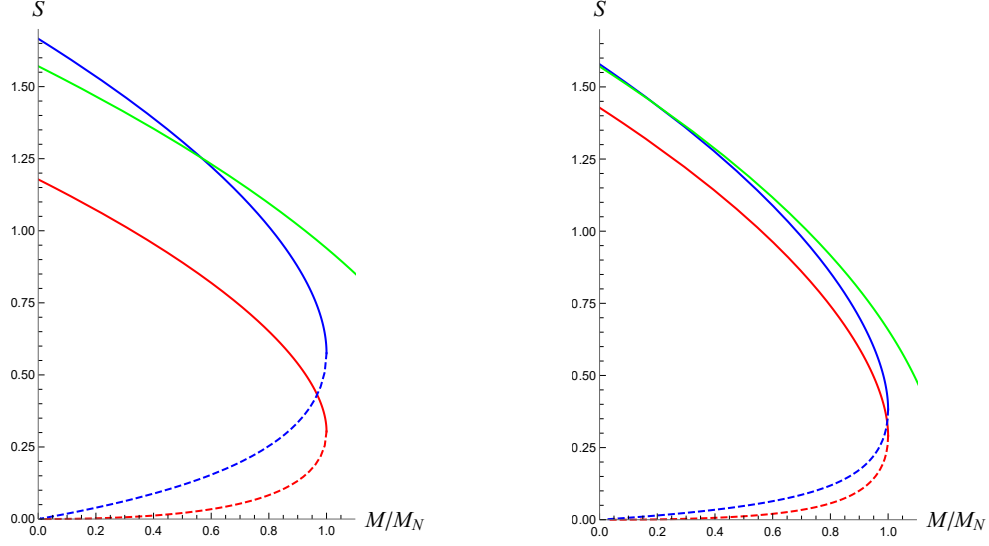


Figure 8: Plot of $S_{\text{gen}}^{(3)}$ (red), $S_{\text{BH}}^{(3)}$ (blue) and S_{SdS_3} (green) as a function of mass M . The dashed curves refer to black hole entropies S_h , while the solid curves denote the entropies associated with the cosmological horizon S_c . The backreaction parameter is $\nu = 1/3$ (left) and $\nu = 1/10$ (right), and $\mathcal{G}_3 = R_3 = 1$. As $\nu \rightarrow 0$, all solid curves collapse to S_{SdS_3} , while the dashed curves go to zero.

which is the same as (3.11), and is proportional to the Gibbons-Hawking entropy of the dS_3 cosmological horizon. As a generalized entropy, this quantity represents the sum of gravitational entropy and entanglement entropy due to the CFT living outside of the cosmological horizon.

Further, the generalized entropy (5.27) is related to the three-dimensional Bekenstein-Hawking entropy $S_{\text{BH}}^{(3)}$ of the horizon(s) on the brane as

$$S_{\text{gen}}^{(3)} = \frac{\sqrt{1-\nu^2}}{1+\nu z} S_{\text{BH}}^{(3)}, \quad (5.29)$$

where $S_{\text{BH}}^{(3)} = \frac{2\pi r + \eta}{4G_3}$. We see $S_{\text{BH}}^{(3)}$ is influenced by the backreaction, thus containing semi-classical quantum effects. In the limit of vanishing backreaction, the black hole horizon disappears and for the cosmological horizon we find $S_{\text{gen},c}^{(3)}$ and $S_{\text{BH},c}^{(3)}$ coincide and are proportional to the temperature T_c (5.18)

$$\lim_{\nu \rightarrow 0} S_{\text{gen},c}^{(3)} = \lim_{\nu \rightarrow 0} S_{\text{BH},c}^{(3)} = \frac{\pi R_3}{G_3} \frac{z_c}{3z_c^2 - 1} = \frac{\pi^2 R_3^2}{G_3} \lim_{\nu \rightarrow 0} T_c = \frac{\pi R_3}{2G_3} \sqrt{1 - 8G_3 M}, \quad (5.30)$$

where to arrive at the last equality we used that the temperature of the cosmological horizon with conical deficit is $T_c|_{\nu=0} = \frac{1}{2\pi R_3} \sqrt{1 - 8G_3 M}$. We recognize the entropy in this limit as the entropy of the classical three-dimensional Schwarzschild-de Sitter solution [37]

$$S_{\text{SdS}_3} = \frac{2\pi r_c^{\text{SdS}_3}}{4G_3}, \quad (5.31)$$

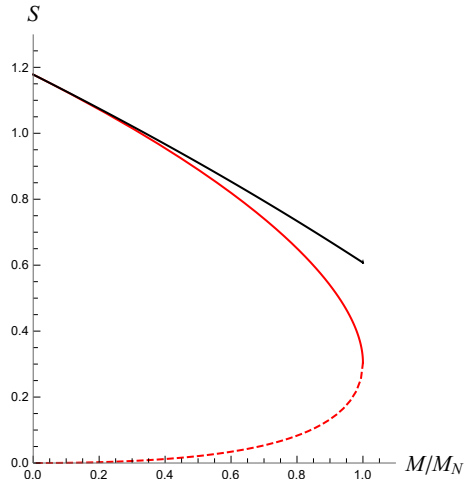


Figure 9: Plot of generalized entropies $S_{\text{gen},h}^{(3)}$ (red dashed curve) and $S_{\text{gen},c}^{(3)}$ (red solid curve) as a function of $\mathcal{M} = M/M_N$. Notice the total generalized entropy $S_{\text{gen,tot}}^{(3)}$ (black), given by the sum of the red solid and dashed curves, is approximately a linear function of the mass. Here we have set $\nu = 1/3$.

with $r_c^{\text{SdS}_3} = R_3 \sqrt{1 - 8G_3 M}$. Finally, in the quantum de Sitter limit ($z = 1$), the area entropy is simply equal to the Gibbons-Hawking entropy

$$S_{\text{BH},c}^{(3)}|_{z=1} = \frac{2\pi R_3}{4G_3} = \frac{2\pi R_3}{4\mathcal{G}_3} \frac{1}{\sqrt{1 - \nu^2}}, \quad (5.32)$$

where \mathcal{G}_3 is the renormalized Newton's constant. Therefore, the Gibbons-Hawking entropy of qdS_3 scales like the classical entropy of dS_3 . A plot of each of these entropies $S_{\text{gen}}^{(3)}$, $S_{\text{BH}}^{(3)}$, and S_{SdS_3} is given in Fig. 8. We observe that the sum of the black hole and cosmological horizon entropies $S_{\text{gen},h}^{(3)}$ and $S_{\text{gen},c}^{(3)}$ produces an approximately linear curve always equal to or less than the entropy of the quantum de Sitter solution (5.28), see Fig. 9. This is reminiscent of the observation in [31, 38] for the classical SdS solution that the sum of the horizon entropies is approximately a linear function of the mass. We will return to this point in Sec. 6, as it will prove useful when computing the nucleation rate of quantum dS black holes.

We can read off the leading order effect the CFT has on the Bekenstein-Hawking entropy by computing the difference between $S_{\text{BH}}^{(3)}$ and S_{SdS_3} ,

$$S_{\text{BH}}^{(3)} - S_{\text{SdS}_3} \approx \frac{\nu z(z^2 - 1)}{(3z^2 - 1)} S_{\text{SdS}_3} + \mathcal{O}(\nu^2). \quad (5.33)$$

Recall from the relation between the central charge c and ν (3.19), that $c \approx \frac{\nu R_3}{2G_3}$, and thus the difference is linear in c . It is thus natural to interpret this difference as the leading contribution to the entanglement entropy of the CFT. We will see more evidence of this momentarily.

In addition to the leading order effect in ν , the backreaction of the CFT induces higher curvature corrections, which enter at order $\mathcal{O}(\nu^2)$. From the brane perspective, one computes the gravitational entropy due to this higher curvature corrections using Wald's entropy

functional S_{Wald} [39]

$$S_{\text{Wald}} = -2\pi \int_{\mathcal{H}} dA \frac{\partial \mathcal{L}}{\partial R^{abcd}} \epsilon_{ab} \epsilon_{cd}, \quad (5.34)$$

where $dA = d^{d-2}x \sqrt{q}$ is the area element of a cross-section \mathcal{H} of the horizon, with q_{ab} being the induced metric on the cross-section, \mathcal{L} is the Lagrangian density defining the gravitational theory, and ϵ_{ab} is the binormal to \mathcal{H} . With respect to the induced gravity action (3.18), the gravitational entropy is [40]

$$S_{\text{Wald}}^{(3)} = \frac{1}{4G_3} \int dx \sqrt{q} \left[1 + \ell^2 \left(\frac{3}{4} \tilde{R} - g_{\perp}^{ab} \tilde{R}_{ab} \right) + \mathcal{O}(\ell^4/R_3^6) \right]. \quad (5.35)$$

with $g_{\perp}^{\perp} = g_{bd} - q_{bd}$ being the metric in the directions orthogonal to the horizon. The dominant contribution is the three-dimensional Bekenstein-Hawking entropy

$$S_{\text{Wald}}^{(3)} = \frac{1}{4G_3} \int dx \sqrt{q} = \frac{1}{4G_3} \int_0^{2\pi} d\bar{\phi} \bar{r}_+ = S_{\text{BH}}^{(3)}, \quad (5.36)$$

as expected. Evaluating (5.35) on the qSdS background $(\bar{t}, \bar{r}, \bar{\phi})$, yields

$$S_{\text{Wald}}^{(3)} = \left[1 + \frac{\nu^2}{2} - \nu^3 \frac{z(z^2 - 1)}{(1 + \nu z)} + \mathcal{O}(\nu^4) \right] S_{\text{BH}}^{(3)}. \quad (5.37)$$

Clearly, in the limit of no backreaction, $S_{\text{Wald}}^{(3)}$ reduces to $S_{\text{BH}}^{(3)}$. Also notice the leading order higher curvature contributions are of order $\mathcal{O}(\nu^2)$, in contrast to the linear order effect of the CFT in (5.33).

It is well known that the generalized entropy is equal to the sum of the gravitational (Wald) entropy plus the fine-grained entropy of matter S_{out} outside of the horizon. We can compute the three-dimensional matter entropy $S_{\text{out}}^{(3)}$ by taking the difference of $S_{\text{gen}}^{(3)}$ (5.29) and the Wald entropy (5.37). To leading order in ν we have,

$$S_{\text{out}}^{(3)} = S_{\text{gen}}^{(3)} - S_{\text{Wald}}^{(3)} \approx -\nu z S_{\text{BH}}^{(3)}. \quad (5.38)$$

Since this quantity is linear in ν , we see it is proportional to central charge c . Notice for large z but fixed $\nu z \ll 1$ we find

$$S_{\text{out}}^{(3)} \approx -\frac{2\pi c}{3}, \quad (5.39)$$

identical to what was found for the qBTZ geometry [6]. As in that case, the overall minus sign does not imply the von Neumann entropy of the CFT is negative. Rather, $S_{\text{out}}^{(3)}$ only corresponds to the finite contribution to the CFT entropy upon absorbing the leading term in the renormalization of G_3 .

First law

Putting together the mass (5.8), temperature (5.16) and entropy (5.26) for the black hole horizon, we find

$$\partial_z M = T_h \partial_z S_{\text{gen},h}^{(3)}. \quad (5.40)$$

Keeping all other parameters fixed, we thus have the first law of (semi-classical) black hole thermodynamics

$$dM = T_h dS_{\text{gen},h}^{(3)} . \quad (5.41)$$

Similarly, for the cosmological horizon we have

$$dM = -T_c dS_{\text{gen},c}^{(3)} . \quad (5.42)$$

Combining these variational relations we attain

$$0 = T_h dS_{\text{gen},h}^{(3)} + T_c dS_{\text{gen},c}^{(3)} . \quad (5.43)$$

Thus, the thermodynamic quantities for either the black hole or cosmological horizon are not independent. Specifically, as the generalized entropy associated with the black hole increases, the generalized entropy attributed to the cosmological horizon decreases. Further, the minus sign in the first law for the cosmological horizon (5.42) indicates the entropy of the cosmological horizon decreases as the mass increases. Consequently, the (generalized) entropy of quantum dS₃ is a maximum entropy configuration such that qdS₃ is an equilibrium state with a *finite* number of degrees of freedom.

Each of the first laws (5.41), (5.42), and (5.43) are precisely what happens for classical higher dimensional SdS, except here the classical entropies $S_{h,c}$ have been replaced by their generalized counterparts $S_{\text{gen},h,c}$. The semi-classical first laws above also hold in the two-dimensional context, where one considers de Sitter JT gravity [14]. Consistent with the thermodynamics of the quantum BTZ solution [6], our observations here provide further evidence that, when semi-classical backreaction is accounted for, quantum black holes obey a first law of thermodynamics where the classical entropy is replaced by the generalized entropy. Additionally, we see the usual but peculiar minus sign in front of the cosmological first law (5.42) is present even when backreaction is accounted for, implying the thermodynamic interpretation of the minus sign is not resolved due to semi-classical modifications.

6 Entropy deficit and nucleation rate of quantum dS black holes

As with black holes, one expects the thermodynamics of the dS cosmological horizon to have a microscopic interpretation. A complete understanding of de Sitter geometry is a task for full-fledged quantum gravity, however, a promising explanation is offered by holography of the dS static patch [41–47]. Recently it was proposed that the dual microscopic theory lives on the (stretched) cosmological horizon [47–49].¹⁴ Evidence for this comes from studying, in particular, the entropy deficit generated by nucleating a four-dimensional classical black hole in de Sitter space, where the nucleation rate is controlled by the deficit. As we will review, the

¹⁴There is another picture of static patch holography, where the dual quantum theory lives on a holographic screen near the north or south poles of the static patch [43, 44]. The two proposals are consistent if the cosmological horizon represents the IR of the underlying microscopic theory while the screen near the poles represents the UV [45].

form of the entropy deficit suggests dS gravity has a matrix theory interpretation [48, 50, 51], and the de Sitter static patch behaves as a holographic quantum mechanical system whose degrees of freedom are localized at the horizon.

It is natural to wonder how well this viewpoint holds up in higher and lower dimensions and when quantum backreaction is accounted for. Here we compare and contrast the central points of [48] for classical de Sitter black holes with the qSdS solution. Importantly, we will see the entropy deficit of a quantum SdS black hole takes on a similar form as its classical four-dimensional counterpart, however, where the classical Bekenstein-Hawking entropy is replaced by the generalized entropy. Moreover, using the fact that the generalized entropy is a linear function of the mass, we compute the nucleation rate using the method of constrained instantons, extending [31] to the case when the backreaction of quantum fields is included.

6.1 Entropy deficit

Consider first the case of classical black holes. Let S_0 denote the entropy of four-dimensional de Sitter space in the static patch

$$S_0 = \frac{4\pi R_4^2}{4G_4}, \quad (6.1)$$

where R_4 is the length scale of dS₄. This entropy is understood to be the entropy when de Sitter space is in thermal equilibrium, such that S_0 is maximized at a given average energy. Fluctuations may arise and shrink the cosmological horizon so that the entropy becomes less than S_0 . Denote this smaller entropy by S_1 . The probability \mathcal{P} of such fluctuations depends on the entropy deficit $\Delta S = S_0 - S_1$,

$$\mathcal{P} \sim e^{-\Delta S}. \quad (6.2)$$

For example, consider a fluctuation in which a small black hole with horizon radius r_+ and mass M appears in dS₄. The geometry is given by the standard four-dimensional Schwarzschild-de Sitter solution

$$ds^2 = -f(r)dt^2 + f^{-1}(r)dr^2 + r^2d\Omega_2^2, \quad f(r) = 1 - \frac{r^2}{R_4^2} - \frac{2MG_4}{r}, \quad (6.3)$$

where ‘small’ here implies $r_+ \ll R_4$. To lowest order in M , the horizon radius is $r_+ = R_4 - MG_4$, and the subsequent entropy S is

$$S = S_0 - 2\pi R_4 M = S_1, \quad (6.4)$$

where in the last equality we identified the entropy $S = S_1$ since including a black hole lowers the entropy of de Sitter space. The entropy deficit ΔS is then

$$\Delta S = 2\pi R_4 M = \sqrt{S_0 s}, \quad (6.5)$$

where $s = 4\pi M^2 G_4$ is the entropy of a four-dimensional flat space Schwarzschild black hole.

More generally, for d -dimensional de Sitter black holes, where now

$$f(r) = 1 - \frac{r^2}{R_d^2} - \frac{16\pi G_d M}{(d-2)\Omega_{d-2} r^{d-3}}, \quad \Omega_{d-2} = \frac{2\pi^{(d-1)/2}}{\Gamma[(d-1)/2]}, \quad (6.6)$$

and R_d is the d -dimensional de Sitter radius, the entropy deficit (6.5) for $s \ll S_0$ becomes

$$\Delta S = 2\pi R_d M = \left(\frac{d-2}{2}\right) S_0^{\frac{1}{d-2}} s^{\frac{d-3}{d-2}}. \quad (6.7)$$

Here s is now the entropy of a d -dimensional (flat space) Schwarzschild black hole.

Expressing the entropy deficit as $\Delta S = \sqrt{S_0 s}$ is interesting in that it depends on the entropies of two systems: the black hole and cosmological horizons. Motivated by [50], ref. [48] argued the entropy deficit (6.5) is reproduced by M(atr)ix theory [52], such that the holographic degrees of freedom of de Sitter space may be represented by $N \times N$ Hermitian matrices, and the entropy deficit (6.5) follows in a straightforward way (up to an overall factor of two).¹⁵

Matrix model description of quantum black holes

We see that the entropy deficit for classical black holes (6.7) does not allow us to consider the three-dimensional case. In the limit of $d = 3$, one has $\Delta S = S_0/2$, where S_0 is the entropy of empty dS_3 . It is clear that the dependence on s vanishes since there are no classical black holes in dS_3 . However, our construction allows us to have such black holes, when they are immersed into quantum fields. Two questions naturally arise: what is the entropy deficit when backreaction is accounted for, and does it have a similar matrix model interpretation?

Clearly, the entropy deficit of nucleating a quantum SdS black hole in (quantum) de Sitter will account for the entropy of quantum fields, as they make a non-negligible contribution to the overall state. Heuristically, we expect the entropy deficit to be related to a difference in generalized entropies,

$$\Delta S_{\text{gen}}^{(3)} = S_{\text{gen},0}^{(3)} - S_{\text{gen}}^{(3)}, \quad (6.8)$$

where $S_{\text{gen},0}^{(3)}$ is the entropy of the dS_3 cosmological horizon including quantum fields (the analog of S_0), and $S_{\text{gen}}^{(3)}$ denotes the entropy of nucleating a small quantum SdS black hole (the analog of S_1). This deficit may be computed explicitly (see App. D for details), however, using braneworld holography we may deduce what to expect.

Holographically, the three-dimensional generalized entropy of the backreacted geometry on the brane is identified with the classical four-dimensional Bekenstein-Hawking entropy of the bulk solution,

$$S_{\text{BH}}^{(4)} \equiv S_{\text{gen}}^{(3)}. \quad (6.9)$$

¹⁵The entropy deficit for d -dimensional systems (6.7) may also be given a matrix model interpretation, however, doing so requires the entropy per degree of freedom to depend on the size of $N \times N$ matrix, $\sigma(N) \sim N^{-(d-4)/(d-3)}$ [48], which we see is potentially problematic for $d = 3$.

Without performing an explicit computation, then, we expect the generalized entropy deficit (6.8) will exhibit the same behavior as the classical four-dimensional entropy deficit (6.5),

$$\Delta S_{\text{gen}}^{(3)} \sim \sqrt{S_{\text{gen},0} s_{\text{gen}}}, \quad (6.10)$$

where s_{gen} the generalized entropy for a black hole in three-dimensional flat space. The ‘ \sim ’ denotes the fact that we expect the entropy deficit may depend on a proportionality factor which depends on the relevant scales, namely ℓ and R_3 ; indeed, we find the relevant factor is $(1 + R_3/\ell)^{1/2}$ (see App. D). Comparing the deficit (6.10) to the four-dimensional entropy deficit (6.5), suggests the holographic degrees of freedom of quantum de Sitter space may likewise be represented by $N \times N$ Hermitian matrices, modulo the overall factor.

Similarly, using the fact that the relation between generalized entropy and mass for holographic conformal fields is the same as for a classical horizon in one more dimension,¹⁶ it is natural to extend this modified deficit to arbitrary spacetime dimension,

$$\Delta S_{\text{gen}} = \mathcal{F}(d, \nu) S_{\text{gen},0}^{\frac{1}{d-1}} s_{\text{gen}}^{\frac{d-2}{d-1}}, \quad (6.11)$$

where $\mathcal{F}(d, \nu)$ is some constant factor which depends on the number of dimensions and the backreaction parameter in such a way so that one recovers the classical deficit (6.7). The lesson one can extract from this simple exercise is that quantum fields play a crucial role in computing the entropy deficit. Consequently, backreaction due to quantum fields will affect nucleation rates, as we now describe.

6.2 Nucleation rate

Entropy deficits play a key role in characterizing black hole nucleation rates. For example, consider the entropy deficit of a classical dS black hole of mass M .

$$\Delta S = S_0 - S_{\text{tot}} = \frac{S_0}{3}(1 - y^2). \quad (6.12)$$

Here S_{tot} is sum of the entropies $S_{h,c} = \frac{4\pi r_{h,c}^2}{4G_4}$, and $y \equiv (r_c - r_h)/R_4$ is a dimensionless length distinguishing the black hole and cosmological horizons in SdS. For $0 < M < M_N$, $y \in [-1, 1]$, where $y = 0$ corresponds to the Nariai limit.¹⁷ In [48] it is argued that the probability to nucleate a black hole of *fixed* mass follows from integrating ΔS with respect to y

$$\mathcal{P} \sim \int_0^1 \frac{d^4 y}{R_4^2} e^{-\Delta S(y)} = \left(\frac{3}{S_0} - \frac{9}{S_0^2} \right) + \frac{9}{S_0^2} e^{-S_0/3}. \quad (6.13)$$

Expressing $S_0 = \pi R_4^2/G_4$, one sees the term between brackets is perturbative in G_4 and accounts for the non-universal microphysics of small black holes. Meanwhile, the second term

¹⁶We are ignoring the effects of possible additional compact dimensions, $AdS \times \mathcal{M}$.

¹⁷Each range $y \in [-1, 0]$ and $y \in [0, 1]$ can be viewed as physically distinct configurations: for $y < 0$, the black hole horizon grows while the cosmological horizon shrinks, until eventually $r_h = r_c$ (the Nariai limit), while for $y > 0$ the horizons swap roles, such that $r_c > r_h$.

is non-perturbative in G_4 but is universal, representing a saddle point when the integrand is at $y = 0$, and thus characterizes a contribution from the Nariai geometry.

While it is intuitive to motivate the nucleation rate (6.13) in terms of the entropy deficit, the above calculation is unsatisfactory for two reasons. First, the parameter y is not well physically motivated and expressing ΔS in terms of y for higher dimensional black holes is technically challenging. Second, the nucleation rate above assumes a fixed mass, but one is generally interested in the nucleation of arbitrary mass black holes. Further, black hole nucleation may be naturally understood as a quantum tunneling process, analogous to bubble nucleation in vacuum decay *viz* Coleman and de Luccia [53].

Therefore, below we advocate computing the nucleation rate via the difference between the on-shell Euclidean action of two different spacetimes. The benefit of this approach not only resolves the aforementioned points (reviewed briefly below), but also easily applies to the quantum black hole case, allowing us to interpret Euclidean qSdS as a “constrained instanton”, and show the nucleation rate is controlled by ΔS_{gen} .

Nucleation of classical dS black holes

In general, one encounters an immediate obstruction in applying the on-shell action method for de Sitter black hole nucleation. The reason is that the Euclideanized SdS background has two conical singularities, one for each horizon. Thus, while one conical singularity may be removed via an appropriate identification of the Euclideanized time coordinate $\tau = it$, there will remain a conical singularity.¹⁸ However, for $d = 4$ [54] and $d \geq 4$ [31], it was shown the on-shell Euclidean action of the SdS solution is

$$I_{\text{E,SdS}} = -(S_h + S_c) = -S_{\text{tot}} . \quad (6.14)$$

This holds for an arbitrary periodicity β of the Euclidean time. Now, an important feature of the total gravitational entropy (6.14) of the SdS solution is that, in any dimension, it is approximately a linear function of the mass M with a negative slope for $M \in [0, M_N]$,

$$S_{\text{tot}} \approx S_0 - (S_0 - S_N) \frac{M}{M_N} , \quad (6.15)$$

with S_0 being the usual entropy of the cosmological horizon in empty de Sitter space.

Heuristically then, the nucleation rate for a black hole of mass M to spontaneously appear in empty de Sitter is given by

$$\mathcal{P} \sim e^{-(I_{\text{E,SdS}} - I_{\text{E,dS}})} \sim e^{-\Delta S} , \quad (6.16)$$

where the second equality follows from using that $I_{\text{E,SdS}}(M = 0) = I_{\text{dS}} = -S_0$. The linear approximation (6.15) resolves the technical challenge of using the parameter y for higher dimensional black holes.

¹⁸Two special cases where there is only a single conical singularity include: (i) pure de Sitter space, where $M = 0$, and where $\tau \sim \tau + \beta_{\text{GH}}$, and (ii) the Nariai geometry, where $\beta_h = \beta_c = \beta_N$, such that $\tau \sim \tau + \beta_N$.

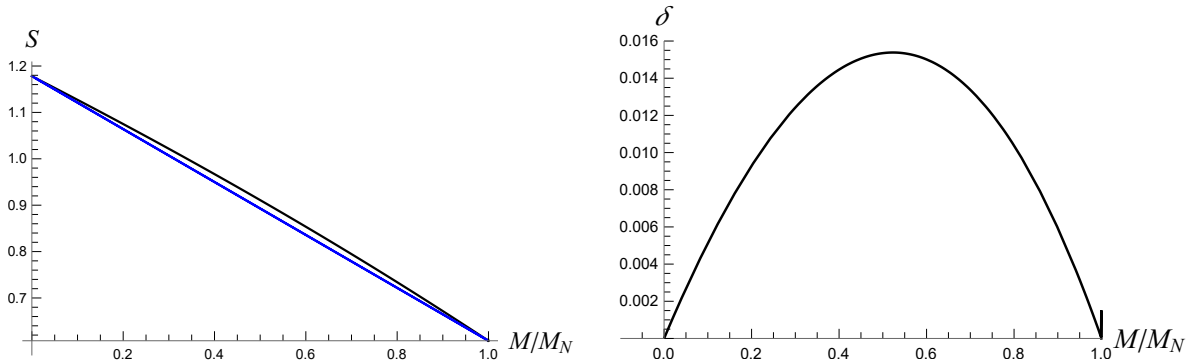


Figure 10: **Left:** Total generalized entropy (black) and its linear fit (blue). **Right:** Difference δ between the total generalized entropy and the linear fit. Here we have set $\nu = 1/3$.

Importantly, the probability (6.16) follows from a Euclidean path integral, where Euclidean SdS black holes represent constrained instantons [31, 55, 56]. More carefully, it is natural to expect the nucleation rate to be described by instanton effects, particularly given the non-perturbative behavior expressed in (6.13). However, it is not a standard instanton, i.e., it is not a solution to the classical Euclidean equations of motion. Rather, the Euclidean SdS geometry is a “constrained instanton”: a stationary point of the Euclidean action when a particular constraint is imposed, namely, fixing the mass. Consequently, the probability rate of creating an arbitrary mass black hole in de Sitter is computed semi-classically via [31]

$$\mathcal{P} \sim \int_0^{M_N} dM e^{-\Delta S} . \quad (6.17)$$

Implementing the linear approximation (6.15), such that $\Delta S = (S_0 - S_N) \frac{M}{M_N}$, the integral (6.17) may be precisely evaluated leading to

$$\mathcal{P} \sim \frac{M_N}{S_0 - S_N} \left[1 - e^{-(S_0 - S_N)} \right] = \frac{M_N}{S_0/3} \left(1 - e^{-S_0/3} \right) , \quad (6.18)$$

This is fairly different from (6.13), because we integrated $e^{-\Delta S}$ over M instead of over y . The pair creation rate (6.18) has a constant contribution and a non-perturbative term coming from the Nariai instanton, but we note the non-perturbative contribution has a factor $3/S_0$ in front instead of $9/S_0^2$ as in (6.13). The overall factor M_N appears so that \mathcal{P} has the dimensions of a probability rate per Hubble volume.

Nucleation of quantum dS black holes

Given our holographic set-up, we expect the qSdS solution to likewise behave as a constrained instanton, such that the probability of nucleation is

$$\begin{aligned} \mathcal{P} &\sim \int_0^{M_N} dM e^{-(I_{E,\text{qSdS}} - I_{E,\text{qdS}})} \approx \int_0^{M_N} dM e^{-\Delta S_{\text{gen}}^{(3)}} \\ &\approx \frac{M_N}{S_{\text{gen},0}^{(3)} - S_{\text{gen},N}^{(3)}} \left[1 - e^{-(S_{\text{gen},0}^{(3)} - S_{\text{gen},N}^{(3)})} \right], \end{aligned} \quad (6.19)$$

analogous to (6.18).

The second equality technically follows from computing the on-shell Euclidean action of the effective three-dimensional theory (3.18).¹⁹ Meanwhile, the final equality follows because, as in the classical case, the total entropy generalized entropy is nearly linear in M/M_N (Fig. 9). Thus, we find the total generalized entropy is well approximated by the linear fit

$$S_{\text{gen}}^{(3),\text{tot}} \approx S_{\text{gen},0}^{(3)} - (S_{\text{gen},0}^{(3)} - S_{\text{gen},N}^{(3)}) \frac{M}{M_N}, \quad (6.20)$$

analogous to (6.15) (see Fig. 10).

Therefore, the entropy deficit is approximately

$$\Delta S_{\text{gen}}^{(3)} \approx (S_{\text{gen},0}^{(3)} - S_{\text{gen},N}^{(3)}) \frac{M}{M_N}, \quad (6.21)$$

which leads to the final line in (6.19).

7 Comments on the holographic dual of de Sitter

Whether de Sitter spacetimes have a holographic description remains one of the most important outstanding questions in quantum gravity. Inspired by AdS/CFT, multiple and distinct pictures of de Sitter holography have been proposed, including in particular [41, 43, 45, 46, 48, 57–65]. A distinguishing feature of each proposal is where the dual non-gravitational microscopic theory lives. On the one hand, the asymptotic fall-off of dS suggests a dual CFT should reside at asymptotic infinity, the natural analog of standard AdS/CFT, where the dual theory lives at the timelike conformal boundary. Alternatively, to better understand the thermodynamics of cosmological horizons, a natural place to put the dual microscopic theory may be on the (stretched) cosmological horizon, or a York-like “boundary” near the poles. While none of the proposals are fully satisfactory, the contrasting features of each make clear that de Sitter holography is an important open problem.

Given the recent successes of models exhibiting double holography [24, 66–68], it is natural to wonder whether this viewpoint has the ability to address the problem of de Sitter

¹⁹Despite not knowing I_{CFT} explicitly, this can be achieved since the effective gravitational contribution is known exactly (though perturbatively), and I_{CFT} follows via subtracting the gravitational effective action from the known bulk action.

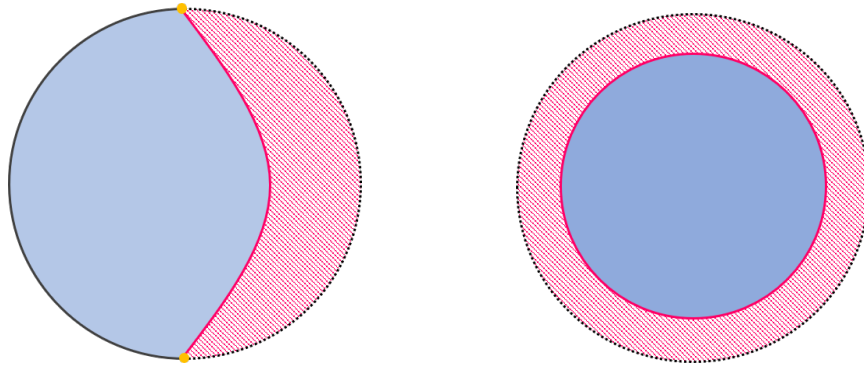


Figure 11: **Left:** An AdS brane embedded into a higher dimensional bulk. The shaded magenta region, including the dashed line of the AdS boundary, has been integrated out. The two points in yellow (a circle, when rotated along the symmetry axis) represent two-dimensional defect CFTs, which are coupled to a bath CFT_3 . The defect CFT is dual to the brane. **Right:** A timeslice of the dS brane embedded into a higher dimensional bulk. The blacked dashed line corresponds to the part of the boundary which has been integrated out, along with the shaded magenta region.

holography. That is, we can ask if the doubly-holographic perspective can shed some light on the nature of a tentative de Sitter dual. Until we find a top-down construction, it is an effective description and will not reveal the ultraviolet holographic degrees of freedom, but perhaps it can help with the question of where these degrees of freedom are located.

Let us first recall how the standard double holography works for AdS branes. In this case, an AdS_d brane hits the conformal boundary of a bulk AdS_{d+1} spacetime at a S^{d-2} that extends in time, as shown in Fig. 11. This sphere corresponds to a defect CFT_{d-1} , which interacts with the bath CFT_d living at the boundary. In the case of an AdS_3 brane, the defect CFT_2 lives on a circle. The reason why this picture is known as double holography is due to the nature of the brane. Namely, the brane dynamics consists of gravity with AdS_d asymptotics, coupled to the same bath CFT_d to which the defect CFT_{d-1} is coupled. The CFT_d on the brane together with its counterpart on the asymptotic boundary allow for a higher dimensional bulk. On the other hand, the AdS_d asymptotics of the brane allow for dualization to a CFT_{d-1} , namely, the defect theory. Therefore, if one was to decouple the defect from the bath, one would simply obtain the usual AdS_3/CFT_2 setup. In other words, we can say that the defect CFT holographically describes the brane.

With a dash of speculation, we can claim that all branes can be sourced in terms of defect CFTs which couple to the bath CFT. What then does such a speculation entail for the de Sitter setup constructed here?

Looking at a generic time slice of our setup, as shown in the right-hand side of Fig. 11, we see that the dS brane appears to be completely independent of the boundary CFT. In other words, it seems as if it does not reach the boundary. Of course, a single snapshot can be misleading, since the dS spacetime is described by an expanding hyperboloid, as shown in Fig. 1. The hyperboloid hits the boundary again at two distinct spheres, but now these are

moments at finite global time. We can easily see this if we transform the metric of AdS₄ in the dS₃ foliation, (3.5), into the conventional global form of AdS₄,

$$ds^2 = -(1 + R^2)dT^2 + \frac{dR^2}{1 + R^2} + R^2d\Omega_2 \quad (7.1)$$

(we set $\ell_4 = 1$ for simplicity), which is obtained from the coordinates in (3.5) by taking

$$T = \arctan \left(\sqrt{1 - \frac{r^2}{R_3^2}} \sinh \frac{t}{R_3} \tanh \sigma \right), \quad (7.2)$$

and

$$R = \sinh \sigma \sqrt{\left(1 - \frac{r^2}{R_3^2}\right) \sinh^2 \frac{t}{R_3} + 1}. \quad (7.3)$$

We see that, along a brane at finite $\sigma = \sigma_b$, the limits $t \rightarrow \pm\infty$ correspond to reaching the boundary $R \rightarrow \infty$ at finite global time $T \rightarrow \pm\pi/2$.

Taking the same perspective as in the case for AdS branes, we see that the analogue of defect CFTs is now played by two Euclidean CFTs, disconnected from the boundary point of view, but connected in the bulk through the brane. In other words, the Euclidean defect CFTs holographically describe the brane, or equivalently, the dual to the de Sitter brane is given by two Euclidean CFTs. Naturally, this picture hints at the dS/CFT construction of [57, 58]. The main difference here lies in the fact that we have two states which source the brane, instead of the usual one-state preparation which fuels the dS phase. Regardless, the two views would seem to be, in terms of calculable observables, equivalent.

A key advantage one might try to extract from our perspective is the possibility of utilizing double holography in our favor. Namely, one can use the higher-dimensional bulk as a means for computing relevant observables, instead of relying on somewhat ill-defined Euclidean CFT computations, as in the usual dS/CFT setup. However, one immediately comes to a halt.

The braneworld setup described here can be interpreted in terms of vacuum decay, as was done in [69] (see also [70, 71]). Recall that vacuum decay from false vacuum to true vacuum *à la* Coleman and de Luccia [53] is understood as a tunneling process through the nucleation of a bubble of true vacuum which then expands and “eats up” the false vacuum. In our picture, the true vacuum is the AdS₄ bulk, the bubble is given by the dS brane, and the false vacuum can be seen as *nothing*.²⁰ Therefore, starting from some $t = 0$ slice in the middle of our hyperboloid, we are evolving towards a fully completed AdS vacuum.

The vacuum decay as described in [53] and [69] leads to a Big Bang/Big Crunch singularity in the past and the future of the Euclidean CFT slices, respectively. One can understand the appearance of the singularity in the following sense: the dS brane is an accelerating brane, and as such it radiates at the quantum level. However, the brane time is infinite, since we are reaching the asymptotic infinities of the dS spacetime. Therefore, the amount of radiation

²⁰Alternatively, one can consider adding Minkowski patches to the sides of the de Sitter hyperboloid, in which case the false vacuum is simply given by Minkowski space.

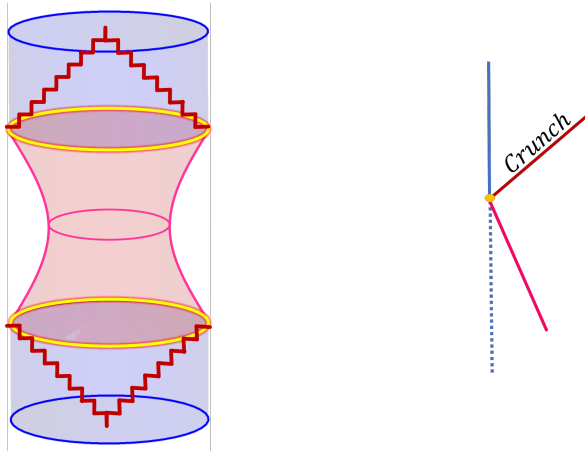


Figure 12: A possible dS/CFT setup via braneworlds. **Left:** Bulk viewpoint. A bulk AdS_{d+1} cylinder (in blue) has a holographic CFT_d dual living at the boundary. The dS_d braneworld, with cutoff surfaces in magenta, lives inside AdS_{d+1} . One might envisage dualizing the dS_d gravity with a Euclidean CFT_{d-1} living at \mathcal{I}^- and \mathcal{I}^+ of the de Sitter hyperboloid (yellow). Bulk quantum corrections are expected to drive the braneworld model to incur big bang and big crunch-like singularities (red), replacing the upper and lower Lorentzian cylinders. Alternatively, one could avoid the singularities altogether by preparing the ‘in’ and ‘out’ states on \mathcal{I}^- and \mathcal{I}^+ via a Euclidean path integral with suitable sources turned on. This would entail replacing the cylinders by appropriate Euclidean submanifolds, closing the contour of the path integral *à la* Schwinger-Keldysh [72–74]. **Right:** The dual quantum mechanical picture, with time running upwards.

such a brane will give off is infinite as well, creating a piling of rays at the future Cauchy horizon, as shown in Fig. 12. Thus, we see that the formation of the singularity is essentially the same phenomenon that enforces Strong Cosmic Censorship at the inner Cauchy horizon in charged or rotating black holes. It will also happen for the past Cauchy horizon.²¹ Hence, it is not clear in what way we can exploit the doubly-holographic setup, since such a singularity might decouple the Euclidean CFTs from the rest of the Lorentzian CFT_3 bath.

Nevertheless, we can take the picture we obtained at face value. The duals claimed here arise as a result of a pure AdS/CFT construction. Therefore, we can see that the AdS/CFT construction itself hints that something like dS/CFT might supply an appropriate notion for a de Sitter dual (if one exists).²² One interesting thing to note is the necessity of correlating

²¹One might wonder why such an event does not happen in usual AdS spacetimes, given that we can have the same dS slicing of empty AdS as well. The key difference lies in the amount of radiation one produces: in order to model the brane radiation, one would need to employ infinite shocks from the boundary in order to produce the same singular effect. Of course, such a state would be pathological to begin with, and so we have no (naturally formed) Big Bang and Big Crunch singularities.

²²One can take this observation a step further (or back) and see a similar story holds for asymptotically flat branes. In that case, the dual would be given in terms of null defects coupled to the Lorentzian bath. There might be subtleties involving high energy shocks from the tip of the null defect, although it is not clear a singularity of the Coleman-de Luccia type would exist. We thank Jamie Sully for emphasizing this point.

the boundary conditions associated to the Euclidean CFTs – otherwise, we would not have an emergent geometry connecting the two theories. Usually, this would be interpreted as a problem for factorization. However, as in the case of low-dimensional AdS/CFT, one might resort to ensemble averaging of some sort in order to deem the correlated boundary conditions more natural. We plan to investigate this viewpoint in the future.

8 Conclusion

While it is well known there are no classical black holes in dS_3 , we have demonstrated quantum backreaction effects can generate a quantum black hole in dS_3 . Our main analysis relied on AdS_4/CFT_3 braneworld holography, where the induced gravity action on a three-dimensional de Sitter brane admits a quantum Schwarzschild de Sitter black hole, with backreaction due to the holographic CFT_3 . A more conventional approach of computing the renormalized stress-tensor due to quantum matter, as carried out in Sec. 2 (and App. B), points to a gravitationally attractive effect that is suggestive of black hole formation. However, this calculation is only reliable to linear order in the Planck length, while our holographic computation holds to all orders in the strength of backreaction (at planar order for the CFT), and therefore the presence of the horizon is well established.

We explored the thermodynamics of the qSdS solution, where we found the solution largely behaves like a classical, four-dimensional SdS black hole; however, importantly, all classical entropies are replaced by their generalized counterparts. In particular, we found it natural to interpret the quantum de Sitter black hole as a non-equilibrium constrained state of a thermodynamic system comprised of a bath (the quantum de Sitter background) and a subsystem (the quantum black hole). Equivalently, the qSdS black hole behaves as a constrained instanton where the probability of nucleating a black hole inside a quantum de Sitter background is controlled by the generalized entropy deficit.

Our thermodynamic analysis also provides insights into the nature of the underlying microscopic degrees of freedom describing the quantum black hole and quantum de Sitter systems. The generalized entropy deficit points to a matrix model description of quantum de Sitter space, where the holographic degrees of freedom of the cosmological horizon are represented by Hermitian matrices, in line with the classical SdS system in four dimensions [48]. In fact, our inclusion of backreaction suggests a quantum generalization of the matrix model conjecture of [48], even in higher dimensions.

A particularly novel feature of our braneworld construction is that it leads to a framework for which we can study dS/CFT . Specifically, the de Sitter gravity theory on the brane is dual to a (defect) Euclidean CFT at \mathcal{I}^- and \mathcal{I}^+ . Advantageously, perhaps, via double-holography one can use the controlled setting of the bulk for computing observables of a typically ill-defined Euclidean CFT.

Lastly, here we focused on quantum dS_3 black holes, a counterpart to the quantum AdS_3 black holes studied in [6]. In the limit of large de Sitter radius R_3 , but finite ℓ , we recover

quantum Schwarzschild black holes, with horizon radius $r_h = \mu\ell$, in asymptotically locally Minkowski space in three dimensions. These solutions were studied in [5, 13].

There are a number of interesting research avenues worth pursuing, as we now describe.

Rotating, charged quantum de Sitter black holes: It is reasonably straightforward to include rotation, thus leading to rotating quantum de Sitter black holes in three dimensions. Similar to the rotating qBTZ solution [6], the starting point would be the rotating AdS₄ C-metric, however, with parameters tuned such that the brane has a positive cosmological constant. With the addition of rotation, it is expected that the quantum Kerr-dS black hole will have a trifecta of correlated horizons (outer and inner black hole horizons and the cosmological horizon), leading to another extremal or “lukewarm” limit [75–77], where the temperatures of the black hole and cosmological horizons coincide and are in principle distinct from the Nariai limit. One may also consider adding charge to the quantum black hole, starting from, for example, the charged AdS₄ C-metric. Although there is no need for counterterms for the Maxwell field in AdS₄, a Maxwell action is nevertheless generated on a brane at finite distance in the bulk [78], which modifies the geometry of the quantum-corrected black hole. On a de Sitter brane, lukewarm and cold charged instantons are expected.

Euclidean action, quasi-local thermodynamics, and stability of quantum de Sitter: A first principles method for analyzing the thermodynamics of black holes is to directly compute the canonical partition function using a saddle-point approximation of the Euclidean gravitational path integral, *à la* Gibbons and Hawking [79]. However, the standard treatment by Gibbons-Hawking suffers from ambiguities for de Sitter spacetime, since Euclidean de Sitter has no asymptotic boundary where a temperature may be specified to define the canonical ensemble (see [80] for an in depth discussion on this point). Alternatively, one may adapt the quasi-local formalism of York [81] to de Sitter backgrounds and analyze quasi-local thermodynamics. This was recently accomplished in two-dimensional de Sitter JT gravity [14], where backreaction was accounted for exactly and the cosmological system was found to have a negative heat capacity and is thus thermodynamically unstable. It would be interesting to carry out a similar analysis for the quantum SdS solution, and see whether quantum de Sitter is thermodynamically stable.

Holographic complexity in quantum de Sitter space: Models of double holography have recently been used to explore various proposals for information theoretic descriptions of quantum gravity. In particular, the ‘complexity=volume’ and ‘complexity=action’ conjectures have been analyzed in braneworld models [68], where the braneworld gravity was given a holographic description in terms of a defect CFT. More recently, the effects of quantum backreaction were accounted for in these braneworld scenarios in the context of the quantum BTZ black hole [82], with the ‘complexity=volume’ being considerably more favorable over the ‘complexity=action’ scenario. Thus far, however, little attention has been given to studying complexity in de Sitter space (see, *e.g.*, [83–85]). It would be very interesting to see whether the braneworld setup developed here could be used to efficiently study the

aforementioned proposals in a quantum de Sitter background where backreaction effects are incorporated, analogous to the qBTZ analysis [82]. Doing so would require a better understanding of the relation between the dual CFT_3 , and the defect ECFT_2 replacing the gravity on the dS_3 brane. Alternatively, our picture of de Sitter braneworlds, may, in principle, be naturally incorporated into the description of complexity in terms of holographic state preparation [86–88], where complexity may be understood as the minimum number of ‘Lorentzian threads’ attached to unitaries preparing a tensor network state. From this perspective, the de Sitter hyperboloid would represent the time evolution of a dual boundary state prepared by a Euclidean path integral, replacing the standard Lorentzian AdS cylinder. Nonetheless, Lorentzian threads can just as easily extend through the hyperboloid, the number density of which is expected to capture a measure of complexity, leading to a possible connection to the tensor network construction of de Sitter space advocated in [89].

Entanglement wedge islands and radiation entropy: Braneworlds and models of double holography act as a useful arena to study the black hole information paradox, by computing the fine grained entropy of Hawking radiation using the ‘island rule’ [24, 67, 90], an extremization prescription of semi-classical generalized entropy. Analogous information paradoxes arise in cosmological and de Sitter backgrounds [91–93], where quantum extremal surfaces and islands play a key role. Since the qSdS solution uncovered here naturally incorporates the effect of backreaction, we have analytic control over the extremization of the generalized entropy on the brane to study detailed aspects of quantum extremal islands in dS.

Acknowledgments

We are grateful to Ahmed Almheiri, José Barbón, Raphael Bousso, Adam Brown, Jaume Garriaga, Ruth Gregory, Tom Hartman, Matthew Headrick, Christopher Herzog, Stefan Hollands, Kristan Jensen, Juan Maldacena, Alexey Milekhin, Yasunori Nomura, Edgar Shaghoulian, Eva Silverstein, Jon Sorce, James Sully, Leonard Susskind, and Zhenbin Yang for discussions and useful correspondence. RE is supported by MICINN grant PID2019-105614GB-C22, AGAUR grant 2017-SGR 754, and State Research Agency of MICINN through the ‘Unit of Excellence Maria de Maeztu 2020-2023’ award to the Institute of Cosmos Sciences (CEX2019-000918-M). JFP is supported by the ‘Atracción de Talento’ program (2020-T1/TIC-20495, Comunidad de Madrid) and by the Spanish Research Agency (Agencia Estatal de Investigación) through the Grant IFT Centro de Excelencia Severo Ochoa No. CEX2020-001007-S, funded by MCIN/AEI/10.13039/501100011033. AS is supported by the Simons Foundation via *It from Qubit: Simons Collaboration on quantum fields, gravity, and information*, and EPSRC. MT is supported by the European Research Council (ERC) under the European Union’s Horizon 2020 research and innovation programme (grant agreement No 852386). MV is supported by the Republic and canton of Geneva and the Swiss National Science Foundation, through Project Grants No. 200020-182513 and No. 51NF40-141869 The Mathematics of Physics (SwissMAP). AS and MV acknowledge the University of Barcelona for hospitality

where this work was initiated. RE, JP, AS and MT acknowledge the Galileo Galilei Institute in Arcetri, Italy for its vibrant environment that allowed for fruitful discussions. MT and MV thank the participants of the Peyresq Physics workshop 2022 for useful interactions on this work.

A Gravitational attraction from negative energy

It seems paradoxical that the negative Casimir energy created by a conical defect generates an attractive gravitational potential. However, this is an instance of a wider phenomenon that is present, only in reverse, in a much better known setup, so we will begin with it.

Apparent gravitational repulsion from positive energy

Let us write the Reissner-Nordström solution as

$$ds^2 = - \left(1 - \frac{2\mathcal{M}(r)}{r} \right) dt^2 + \frac{dr^2}{1 - \frac{2\mathcal{M}(r)}{r}} + r^2 d\Omega_2, \quad (\text{A.1})$$

where

$$\mathcal{M}(r) = M - \frac{Q^2}{2r}. \quad (\text{A.2})$$

The function $\mathcal{M}(r)$ can be regarded as the “effective mass” that acts on a neutral test particle at radius r . We see that the electric field of the black hole decreases the gravitational force on such a particle, relative to a neutral black hole with the same mass M . Indeed, the acceleration of a neutral particle at fixed position (following an orbit of ∂_t) is smaller if we increase the charge Q of the background geometry while keeping M fixed. Thus, the electric field would seem to have a repulsive gravitational effect, despite the fact that its energy density,

$$\rho_{el} = -T^t_t = \frac{Q^2}{2r^4}, \quad (\text{A.3})$$

is positive.

The correct interpretation, however, is different. The asymptotic mass M measures the gravitational effect of *all* the energy sources that are inside a sphere at infinity,²³ including also the electromagnetic field energy. Thus, if we put a test particle on the surface of a sphere at finite radius, then the electromagnetic energy that lies outside this sphere will not have any gravitational pull on the particle. When computing the actual mass that attracts the particle at r , the electromagnetic energy outside the sphere of radius r must be subtracted from M , resulting in (A.2).

Thus we see that the apparent repulsive gravitation of the electromagnetic field energy merely reflects a reduced attraction due to the lower energy that is enclosed as we move to spheres of smaller radii.

²³Readers who feel uneasy about the ‘energy sources’ of the non-linear Schwarzschild or Reissner-Nordström solutions can sidestep the issue by linearizing gravity and considering localized mass sources. Our arguments equally go through.

Gravitational attraction from negative Casimir energy in 2 + 1 dimensions

The previous argument easily explains how the negative Casimir energy density (1.4)

$$\rho_{Cas} = -\langle T^t_t \rangle = -\frac{\hbar F(M)}{8\pi r^3} \quad (\text{A.4})$$

gives rise to gravitational attraction. The only subtlety is that, in 2 + 1 dimensions, a classical localized mass does not generate any gravitational attraction itself, only a deficit angle. This deficit, measured on circles at large radii, is related to the mass as in (1.2). In our quantum-corrected solutions, considering for simplicity the asymptotically locally flat limit $R_3 \rightarrow \infty$, we could define an effective mass

$$\mathcal{M}(r) = M + \frac{\hbar F(M)}{4r}, \quad (\text{A.5})$$

which indicates that the quantum corrections enhance the gravitational effects at finite r , not only increasing the deficit angle at finite r , but also accelerating neutral particles towards smaller radii.

We now know how to understand this attraction. The asymptotic mass M measures the gravitational effect of all the energy enclosed in a circle at infinity, including the Casimir energy. The attraction at finite r is a consequence of having less negative energy enclosed in a circle of radius $r < \infty$ than in one at infinity. What makes the effect perhaps more surprising is that in 2 + 1 dimensions the leading asymptotic mass term M does not result in any attraction, while the finite- r correction does. But its origin is the same as we have seen above.

It can easily be seen that the explanation for the effect given in [8] reduces to the argument that we have presented here, only in a more elaborate form (accounting for an explicit mass source near $r = 0$), but which is possibly less transparent.

B Renormalized stress tensor of conical defect in dS_3

Here we provide the details for computing the renormalized quantum stress-energy tensor of a conformally coupled massless scalar field to the Einstein-Hilbert action for a conical defect in dS_3 . Our treatment below follows standard techniques using point-splitting, as described in, for instance, [7, 16, 94].

Conical defect in dS_3

Static, circularly symmetric solutions to the Einstein-Hilbert action in three dimensions with pointlike matter sources and a positive cosmological constant $\Lambda = +1/R_3^2$ may be parameterized as

$$ds^2 = -\left(1 - 8G_3M - \frac{r^2}{R_3^2}\right) dt^2 + \left(1 - 8G_3M - \frac{r^2}{R_3^2}\right)^{-1} dr^2 + r^2 d\phi^2, \quad (\text{B.1})$$

with $-\infty < t < \infty$, $0 \leq r \leq \infty$, and the angular coordinate ϕ is 2π -periodic. The value of M lends two distinct scenarios: (i) $M = 0$ corresponds to pure dS_3 in static patch coordinates with a cosmological horizon $r_c = R_3$, and (ii) for $8G_3M < 1$ we have the Schwarzschild-de Sitter (SdS) solution. Case (ii) does not describe a black hole in dS_3 , but rather a conical defect with a cosmological horizon at $r_c = R_3\sqrt{1 - 8G_3M}$. To see appreciate this point, define the parameter $\gamma^2 \equiv 1 - 8G_3M$, and perform the following coordinate rescaling,

$$\tilde{t} = \gamma t, \quad \tilde{r} = \gamma^{-1}r, \quad \tilde{\phi} = \gamma\phi. \quad (\text{B.2})$$

The dS_3 line element (B.1) becomes

$$ds^2 = -\left(1 - \frac{\tilde{r}^2}{R_3^2}\right) d\tilde{t}^2 + \left(1 - \frac{\tilde{r}^2}{R_3^2}\right)^{-1} d\tilde{r}^2 + \tilde{r}^2 d\tilde{\phi}^2. \quad (\text{B.3})$$

This looks like dS_3 in static patch coordinates, however, with the notable difference that now the angular variable has a different periodicity: $\tilde{\phi} \sim \tilde{\phi} + 2\pi\gamma$. Thus, this spacetime exhibits a conical defect, if $0 \leq \gamma < 1$, with a deficit angle $\delta = 2\pi(1 - \gamma)$. One may interpret this solution as a massive point particle sourcing the curvature, producing a curvature singularity as a delta function source at the pole of the static patch of dS_3 . In fact, a conical deficit at the north pole also induces a conical deficit at the south pole, since timeslices of dS_3 are closed. Hence, conical dS_3 solutions have two point particles, one at each pole.

Finally, we want to compare the metric in (B.1) with the original metric found by Deser-Jackiw to describe two point particles in dS_3 [4]. By performing the following coordinate transformation

$$r = \frac{R_3\gamma}{\cosh(\gamma \ln z)} = \frac{2\gamma R_3}{z^\gamma + z^{-\gamma}}, \quad \text{or} \quad z^\gamma = \frac{\gamma - \sqrt{\gamma^2 - r^2/R_3^2}}{r/R_3}, \quad (\text{B.4})$$

the metric (B.1) of conical dS_3 turns into

$$ds^2 = -\gamma^2 \tanh^2(\gamma \ln z) dt^2 + \frac{\gamma^2 R_3^2 (dz^2 + z^2 d\phi^2)}{z^2 \cosh^2(\gamma \ln z)}, \quad (\text{B.5})$$

$$= -\gamma^2 \left(\frac{z^\gamma - z^{-\gamma}}{z^\gamma + z^{-\gamma}}\right)^2 dt^2 + \frac{4\gamma^2 R_3^2 (dz^2 + z^2 d\phi^2)}{z^2 (z^\gamma + z^{-\gamma})^2}. \quad (\text{B.6})$$

This agrees with the metric which Deser-Jackiw use for conical dS_3 , see Eqs. (3.5) and (3.8) in [4]. For $\gamma = 1$ the spatial part describes a round sphere in stereographic coordinates.

Adding a massless conformally coupled scalar field

Consider a massless scalar field Φ conformally coupled to the Einstein-Hilbert action in three dimensions (2.1), whose classical matter stress-energy tensor $T_{\mu\nu}$ is given by

$$T_{\mu\nu} = \frac{3}{4} \nabla_\mu \Phi \nabla_\nu \Phi - \frac{1}{4} g_{\mu\nu} (\nabla \Phi)^2 - \frac{1}{4} \Phi \nabla_\mu \nabla_\nu \Phi + \frac{1}{4} g_{\mu\nu} \Phi \square \Phi + \xi G_{\mu\nu} \Phi^2, \quad (\text{B.7})$$

where $G_{\mu\nu}$ is the Einstein tensor and $\xi = \frac{1}{8}$. When the background is maximally symmetric we have $G_{\mu\nu} = -g_{\mu\nu}\Lambda$. Meanwhile the scalar field equation of motion is

$$(\square - \xi R)\Phi = 0. \quad (\text{B.8})$$

Here $R = \frac{6}{R_3^2}$ when we are in dS_3 . Upon invoking (B.8), it is straightforward to verify the classical stress-energy tensor (B.7) is traceless and conserved, $g^{\mu\nu}T_{\mu\nu} = \nabla^\mu T_{\mu\nu} = 0$.

The Green function $G_{\text{CdS}_3}(x, x')$ which solves the scalar field equation of motion (B.8) for a conical defect in dS_3 may be computed using the method of images, analogous to conical AdS_3 [16]. Generically, the Green function $G(x, x')$ with transparent boundary conditions imposed is [17, 18]

$$G(x, x') = \frac{1}{4\pi} \frac{1}{|x - x'|}, \quad (\text{B.9})$$

where $|x - x'| \equiv \sqrt{(x - x')^a (x - x')_a}$ is the chordal or geodesic distance between x and x' in the four-dimensional embedding space $\mathbb{R}^{2,2}$. For pure dS_3 , the embedding coordinates $x^a = (X_1, X_2, T_1, T_2)^T$ are

$$T_1 = \sqrt{r^2 - R_3^2} \cosh(t/R_3), \quad T_2 = \sqrt{r^2 - R_3^2} \sinh(t/R_3), \quad X_1 = r \cos \phi, \quad X_2 = r \sin \phi. \quad (\text{B.10})$$

It is easy to verify

$$-T_1^2 + T_2^2 + X_1^2 + X_2^2 = R_3^2, \quad (\text{B.11})$$

and

$$\begin{aligned} ds^2 &= -dT_1^2 + dT_2^2 + dX_1^2 + dX_2^2 \\ &= -\left(1 - \frac{r^2}{R_3^2}\right) dt^2 + \left(1 - \frac{r^2}{R_3^2}\right)^{-1} dr^2 + r^2 d\phi^2. \end{aligned} \quad (\text{B.12})$$

Then,

$$|x - x'| = \left[2R_3^2 + 2\sqrt{r^2 - R_3^2} \sqrt{r'^2 - R_3^2} \cosh\left(\frac{t - t'}{R_3}\right) - 2rr' \cos(\phi - \phi') \right]^{1/2}. \quad (\text{B.13})$$

Further, one can show

$$\left(\square - \frac{3}{4R_3^2}\right) G_{\text{dS}_3}(x, x') = 0, \quad (\text{B.14})$$

when $x \neq x'$, and where $G_{\text{dS}_3}(x, x')$ refers to the Green function with respect pure dS_3 in static patch coordinates.

One may construct the Green function $G_{\text{CdS}_3}(x, x')$ for the conical defect spacetime (B.3) via the method of images. That is, one uses the fact that the conical defect spacetime corresponds to discrete identifications of dS_3 . Specifically, analogous to the AdS_3 case (see, *e.g.*, [94]), identified points are related by an element $H \in SO(1, 3)$ on the embedding space coordinates (B.10), except where $\phi \sim \phi + 2\pi\gamma$, with $\gamma \equiv 1/N$ for some positive integer N ,

$$H = \begin{pmatrix} \cos(2\pi\gamma) & \sin(2\pi\gamma) & 0 & 0 \\ -\sin(2\pi\gamma) & \cos(2\pi\gamma) & 0 & 0 \\ 0 & 0 & 1 & 1 \\ 0 & 0 & 0 & 1 \end{pmatrix}. \quad (\text{B.15})$$

The Green function $G_{\text{CdS}_3}(x, x')$ for the conical defect spacetime then follows from the image sum

$$G_{\text{CdS}_3}(x, x') = \sum_{n=-\infty}^{\infty} G_{\text{dS}_3}(x, H^n x') = \frac{1}{4\pi} \sum_{n \in \mathbb{Z}} \frac{1}{|x - H^n x'|}, \quad (\text{B.16})$$

with

$$|x - H^n x'| = \left[2R_3^2 + 2\sqrt{r^2 - R_3^2} \sqrt{r'^2 - R_3^2} \cosh\left(\frac{t - t'}{R_3}\right) - 2rr' \cos\left(\phi - \phi' + \frac{2\pi n}{N}\right) \right]^{1/2}. \quad (\text{B.17})$$

Crucially, in the conical defect spacetime, the infinite sum becomes a finite sum,

$$G_{\text{CdS}_3}(x, x') = \frac{1}{4\pi} \sum_{n=0}^{N-1} \frac{1}{|x - H^n x'|}, \quad (\text{B.18})$$

which follows from the fact there exist only a finite number N of geodesics connecting two points on a cone [95]. Upon a Wick rotation $L = iR_3$, one recovers the scalar field Green function in conical AdS₃ [94].

Quantum stress tensor for a conical defect in dS₃

We can now obtain the renormalized quantum stress tensor $\langle T_{\mu\nu} \rangle$ from $G(x, x')$ using the point-splitting method [7, 16, 94, 96, 97]. Specifically,

$$\langle T_{\mu\nu}(x) \rangle = \lim_{x' \rightarrow x} \left(\frac{3}{4} \nabla_\mu^x \nabla_\nu^{x'} G - \frac{1}{4} g_{\mu\nu} g^{\alpha\beta} \nabla_\alpha^x \nabla_\beta^{x'} G - \frac{1}{4} \nabla_\mu^x \nabla_\nu^x G + \frac{1}{16R_3^2} g_{\mu\nu} G \right), \quad (\text{B.19})$$

where $G(x, x') = G_{\text{CdS}_3}(x, x')$ is the Green function (B.18), the metric $g_{\mu\nu}$ is a function of spacetime point x , ∇_μ^x denotes a covariant derivative with respect to point x , and $\nabla_\mu^{x'}$ denotes a derivative with respect to the point x' . Moreover, the limit $x \rightarrow x'$ is the coincident limit, which amounts to evaluating the resulting expression at $x' = x$. Note that while normally the renormalization of the stress tensor is difficult, here one simply subtracts off the $n = 0$ term in the image sum in the coincident limit; indeed, the $n = 0$ term includes the divergent contribution.

To evaluate each component of the renormalized stress tensor in the conical defect background, we recognize $G(x, x')$ is a symmetric biscalar, while its covariant derivatives are examples of bitensors. Consequently, one invokes a generalization of Synge's theorem for bitensors developed by Christensen [96] (also see Eq. (54) of [98]):

$$\lim_{x' \rightarrow x} (\nabla_\mu^{x'} A_{\alpha_1}) = \nabla_\mu^x \lim_{x' \rightarrow x} (A_{\alpha_1}) - \lim_{x' \rightarrow x} (\nabla_\mu^x A_{\alpha_1}), \quad (\text{B.20})$$

where A_{α_1} is a bivector with equal weight at both x and x' , whose coincidence limit exists. Consequently, applying Synge's rule (B.20) to the quantum stress tensor (B.19) we have:

$$\begin{aligned} \langle T_{\mu\nu}(x) \rangle &= \frac{3}{4} \left[\nabla_\nu^x \lim_{x' \rightarrow x} (\nabla_\mu^x G) - \lim_{x' \rightarrow x} (\nabla_\nu^x \nabla_\mu^x G) \right] - \frac{1}{4} g_{\mu\nu} g^{\alpha\beta} \left[\nabla_\beta^x \lim_{x' \rightarrow x} (\nabla_\alpha^x G) - \lim_{x' \rightarrow x} (\nabla_\beta^x \nabla_\alpha^x G) \right] \\ &+ \lim_{x' \rightarrow x} \left(-\frac{1}{4} \nabla_\mu^x \nabla_\nu^x G + \frac{1}{16R_3^2} g_{\mu\nu} G \right). \end{aligned} \quad (\text{B.21})$$

Evaluating this in the conical defect spacetime (B.1), we find all off-diagonal components vanish, leaving only non-zero diagonal contributions (1.4) with form factor $F(\gamma)$ (2.3)

C Bulk dual of a CFT in conical dS₃

Here we show the bulk dual description of a holographic CFT in conical dS₃ is equal to a double Wick rotation of the hyperbolic AdS₄ black hole. To see this, consider the limit of vanishing backreaction $\ell \rightarrow 0$ of the AdS₄ C-metric (4.1),

$$ds^2 = \frac{\ell^2}{x^2 r^2} \left[- \left(1 - \frac{r^2}{R_3^2} \right) dt^2 + \left(1 - \frac{r^2}{R_3^2} \right)^{-1} dr^2 + r^2 (G^{-1}(x) dx^2 + G(x) d\phi^2) \right], \quad (\text{C.1})$$

where $G(x) = 1 - x^2 - \mu x^3$. In the limit $\ell \rightarrow 0$, the AdS₄ cosmological constant yields $\ell_4 = \ell$. Clearly, along boundary $x = 0$, where $G(x) = 1$, the above geometry is conformally equivalent to conical dS₃. Under the following double Wick rotation,

$$t = -iR_3\Phi, \quad r = \frac{R_3}{\cosh u}, \quad x = \frac{1}{\hat{\rho}}, \quad \phi = -i\hat{T}, \quad (\text{C.2})$$

with $u \in \mathbb{R}_+$ and $\Phi \in [0, 2\pi]$, the line element (C.1) becomes

$$ds^2 = \ell_4^2 \left[- \left(\hat{\rho}^2 - 1 - \frac{\mu}{\hat{\rho}} \right) d\hat{T}^2 + \left(\hat{\rho}^2 - 1 - \frac{\mu}{\hat{\rho}} \right)^{-1} d\hat{\rho}^2 + \hat{\rho}^2 (du^2 + \sinh^2(u) d\Phi^2) \right]. \quad (\text{C.3})$$

Observe that when taking the limit $\ell \rightarrow 0$ with R_3 fixed, we are also sending $\ell_4 \rightarrow 0$, so the entire metric shrinks to zero size. We can nevertheless effectively blow up the metric to finite size again by rescaling

$$\hat{\rho} = \frac{\rho}{\ell_4}, \quad \hat{T} = \frac{T}{\ell_4}, \quad \mu = \frac{2mG_4}{\ell_4}. \quad (\text{C.4})$$

Then we recover the line element for the hyperbolic (or topological) AdS₄ black hole [99],

$$ds^2 = -f(\rho) dT^2 + f^{-1}(\rho) d\rho^2 + \rho^2 (du^2 + \sinh^2(u) d\Phi^2), \quad f(\rho) = \frac{\rho^2}{\ell_4^2} - 1 - \frac{2mG_4}{\rho}. \quad (\text{C.5})$$

Here the parameter m is related to the ADM mass M via

$$M = \frac{m\omega_2}{4\pi} = \frac{\omega_2}{8\pi G_4} \rho_+ \left[\left(\frac{\rho_+}{\ell_4} \right)^2 - 1 \right], \quad (\text{C.6})$$

where $\rho = \rho_+$ is the location of the horizon, and $\omega_2 = 2\pi \int_0^\infty \sinh(u) du$ is the volume of hyperbolic space with unit radius. The Bekenstein-Hawking entropy and temperature, meanwhile, are

$$S_{\text{BH}}^{(4)} = \frac{\omega_2 \rho_+^2}{4G_4}, \quad T_{\text{H}} = \frac{1}{4\pi \rho_+} \left(\frac{3\rho_+^2}{\ell_4^2} - 1 \right). \quad (\text{C.7})$$

This gravitational entropy is generally divergent due to the infinite extent of the \mathbb{H}^2 hyperbolic space ω_2 , in accordance with the entanglement entropy of the dual CFT, and may be regulated by introducing a cutoff.

D Entropy deficit of small quantum dS black hole

Consider the generalized entropy (5.26) of the cosmological horizon evaluated about $r_+ = R_3 - \frac{\mu\ell}{2}$ at small μ , where we keep ℓ fixed, but ν is still assumed to be small. Then,

$$S_{\text{gen}}^{(3)} \approx \frac{\pi R_3^2}{2\mathcal{G}_3(\ell + R_3)} - \frac{\pi R_3 \mu \ell}{2\mathcal{G}_3(\ell + R_3)} + \mathcal{O}(\mu^2), \quad (\text{D.1})$$

where we used $x_1 \approx 1$ at small μ . In the limit $\ell \rightarrow 0$, we find $S_{\text{gen}}^{(3)} = \frac{\pi R_3}{2\mathcal{G}_3}$, the entropy of empty dS₃. The entropy (D.1) is the analog of the classical entropy S_1 and is less than the maximum entropy $S_{\text{gen},0}^{(3)} = \frac{\pi R_3^2}{2\mathcal{G}_3(\ell + R_3)}$, the entropy of the cosmological horizon of dS₃ including matter field fields (5.28). The entropy deficit $\Delta S_{\text{gen}}^{(3)}$ is therefore,

$$\Delta S_{\text{gen}}^{(3)} = S_{\text{gen},0}^{(3)} - S_{\text{gen}}^{(3)} \approx \frac{\pi R_3 \mu \ell}{2\mathcal{G}_3(\ell + R_3)} \approx 2\pi R_3 M, \quad (\text{D.2})$$

where in the last equality we used that $M \approx \frac{\mu\ell}{4\mathcal{G}_3(\ell + R_3)}$ in the limit $r_+ = R_3 - \frac{\mu\ell}{2}$ for small μ .

We observe the deficit of the generalized entropy for the qSdS solution is precisely of the same form as the classical entropy deficit (6.5), however, here the deficit vanishes in the case of vanishing backreaction. Note that had we instead considered a conical deficit in three-dimensional de Sitter space, the form of the entropy deficit would be the same, where the mass M would be identified with the ‘mass’ of the conical defect.

Further, we may write the deficit as

$$\Delta S_{\text{gen}}^{(3)} = S_{\text{dS}_3}(2\mathcal{G}_3 M), \quad (\text{D.3})$$

with $S_{\text{dS}_3} = \frac{2\pi R_3}{2\mathcal{G}_3}$. This is the analog of the classical four-dimensional result (6.5). Alternatively, the generalized entropy of a small black hole s_{gen} is proportional to M^2 . To see this, note that the black hole horizon of our qSdS black hole increases linearly in $\mu\ell$. This follows from expanding (4.16) about $r_h = 0$, such that at leading order,

$$R_3^2 \approx r_c^2 \left(1 + \frac{r_h}{r_c} \right), \quad \mu\ell \approx r_h. \quad (\text{D.4})$$

Then, let s_{gen} denote the value of $S_{\text{gen}}^{(3)}$ evaluated at $r_+ \approx \mu\ell$, expanded about small μ ,

$$s_{\text{gen}} \equiv S_{\text{gen}}^{(3)}|_{r_+=\mu\ell} \approx \frac{\ell\pi\mu^2}{2\mathcal{G}_3}. \quad (\text{D.5})$$

Notice s_{gen} vanishes in the limit of zero backreaction, as expected. Further, the mass M (5.8) goes as

$$M|_{r_+=\mu\ell} \approx \frac{\mu}{4\mathcal{G}_3}, \quad (\text{D.6})$$

such that

$$\frac{s_{\text{gen}}}{8\pi\mathcal{G}_3\ell} = M^2. \quad (\text{D.7})$$

Consequently, we may alternatively recast the entropy deficit (D.2) as

$$\Delta S_{\text{gen}}^{(3)} = \sqrt{(1 + R_3/\ell)S_{\text{gen},0}^{(3)}}. \quad (\text{D.8})$$

which has a similar form as the four-dimensional deficit (6.5).

References

- [1] S. Deser, R. Jackiw and G. 't Hooft, *Three-Dimensional Einstein Gravity: Dynamics of Flat Space*, *Annals Phys.* **152** (1984) 220.
- [2] M. Banados, C. Teitelboim and J. Zanelli, *The Black hole in three-dimensional space-time*, *Phys. Rev. Lett.* **69** (1992) 1849–1851, [[hep-th/9204099](#)].
- [3] M. Banados, M. Henneaux, C. Teitelboim and J. Zanelli, *Geometry of the (2+1) black hole*, *Phys. Rev. D* **48** (1993) 1506–1525, [[gr-qc/9302012](#)].
- [4] S. Deser and R. Jackiw, *Three-Dimensional Cosmological Gravity: Dynamics of Constant Curvature*, *Annals Phys.* **153** (1984) 405–416.
- [5] R. Emparan, A. Fabbri and N. Kaloper, *Quantum black holes as holograms in AdS brane worlds*, *JHEP* **08** (2002) 043, [[hep-th/0206155](#)].
- [6] R. Emparan, A. M. Frassino and B. Way, *Quantum BTZ black hole*, *JHEP* **11** (2020) 137, [[2007.15999](#)].
- [7] T. Souradeep and V. Sahni, *Quantum effects near a point mass in (2+1)-Dimensional gravity*, *Phys. Rev. D* **46** (1992) 1616–1633, [[hep-ph/9208219](#)].
- [8] H. H. Soleng, *Inverse square law of gravitation in (2+1) dimensional space-time as a consequence of Casimir energy*, *Phys. Scripta* **48** (1993) 649–652, [[gr-qc/9310007](#)].
- [9] P. Bueno, R. Emparan and Q. Llorens, *Higher-curvature Gravities from Braneworlds and the Holographic c-theorem*, [2204.13421](#).
- [10] S. de Buyl, S. Detournay, G. Giribet and G. S. Ng, *Baby de Sitter black holes and dS₃/CFT₂*, *JHEP* **02** (2014) 020, [[1308.5569](#)].
- [11] H. Nariai, *On a new cosmological solution of einstein’s field equations of gravitation*, *General relativity and gravitation* **31** (06, 1999) 963 – 971.
- [12] P. H. Ginsparg and M. J. Perry, *Semiclassical Perdurance of de Sitter Space*, *Nucl. Phys. B* **222** (1983) 245–268.
- [13] R. Emparan, *Black hole entropy as entanglement entropy: A Holographic derivation*, *JHEP* **06** (2006) 012, [[hep-th/0603081](#)].
- [14] A. Svesko, E. Verheijden, E. P. Verlinde and M. R. Visser, *Quasi-local energy and microcanonical entropy in two-dimensional nearly de Sitter gravity*, [2203.00700](#).
- [15] G. W. Gibbons and S. W. Hawking, *Cosmological Event Horizons, Thermodynamics, and Particle Creation*, *Phys. Rev. D* **15** (1977) 2738–2751.
- [16] A. R. Steif, *The Quantum stress tensor in the three-dimensional black hole*, *Phys. Rev. D* **49** (1994) 585–589, [[gr-qc/9308032](#)].

- [17] S. J. Avis, C. J. Isham and D. Storey, *Quantum Field Theory in anti-De Sitter Space-Time*, *Phys. Rev. D* **18** (1978) 3565.
- [18] G. Lifschytz and M. Ortiz, *Scalar field quantization on the (2+1)-dimensional black hole background*, *Phys. Rev. D* **49** (1994) 1929–1943, [[gr-qc/9310008](#)].
- [19] C. Martinez and J. Zanelli, *Conformally dressed black hole in (2+1)-dimensions*, *Phys. Rev. D* **54** (1996) 3830–3833, [[gr-qc/9604021](#)].
- [20] C. Martinez and J. Zanelli, *Back reaction of a conformal field on a three-dimensional black hole*, *Phys. Rev. D* **55** (1997) 3642–3646, [[gr-qc/9610050](#)].
- [21] L. Randall and R. Sundrum, *A Large mass hierarchy from a small extra dimension*, *Phys. Rev. Lett.* **83** (1999) 3370–3373, [[hep-ph/9905221](#)].
- [22] L. Randall and R. Sundrum, *An Alternative to compactification*, *Phys. Rev. Lett.* **83** (1999) 4690–4693, [[hep-th/9906064](#)].
- [23] S. de Haro, K. Skenderis and S. N. Solodukhin, *Gravity in warped compactifications and the holographic stress tensor*, *Class. Quant. Grav.* **18** (2001) 3171–3180, [[hep-th/0011230](#)].
- [24] H. Z. Chen, R. C. Myers, D. Neuenfeld, I. A. Reyes and J. Sandor, *Quantum Extremal Islands Made Easy, Part I: Entanglement on the Brane*, *JHEP* **10** (2020) 166, [[2006.04851](#)].
- [25] J. F. Plebanski and M. Demianski, *Rotating, charged, and uniformly accelerating mass in general relativity*, *Annals Phys.* **98** (1976) 98–127.
- [26] R. Emparan, G. T. Horowitz and R. C. Myers, *Exact description of black holes on branes*, *JHEP* **01** (2000) 007, [[hep-th/9911043](#)].
- [27] R. Emparan, G. T. Horowitz and R. C. Myers, *Exact description of black holes on branes. 2. Comparison with BTZ black holes and black strings*, *JHEP* **01** (2000) 021, [[hep-th/9912135](#)].
- [28] S. Cremonini, J. T. Liu and P. Szepietowski, *Higher Derivative Corrections to R-charged Black Holes: Boundary Counterterms and the Mass-Charge Relation*, *JHEP* **03** (2010) 042, [[0910.5159](#)].
- [29] F. Kottler, *Über die physikalischen Grundlagen der einsteinschen gravitationstheorie*, *Annalen der Physik* **361** (03, 2006) 401 – 462.
- [30] T. R. Choudhury and T. Padmanabhan, *Concept of temperature in multi-horizon spacetimes: Analysis of Schwarzschild-de Sitter metric*, *Gen. Rel. Grav.* **39** (2007) 1789–1811, [[gr-qc/0404091](#)].
- [31] E. K. Morvan, J. P. van der Schaar and M. R. Visser, *On the Euclidean Action of de Sitter Black Holes and Constrained Instantons*, [2203.06155](#).
- [32] G. T. Horowitz and H. J. Sheinblatt, *Tests of cosmic censorship in the Ernst space-time*, *Phys. Rev. D* **55** (1997) 650–657, [[gr-qc/9607027](#)].
- [33] O. J. C. Dias and J. P. S. Lemos, *The extremal limits of the C metric: Nariai, Bertotti-robinson and anti-Nariai C metrics*, *Phys. Rev. D* **68** (2003) 104010, [[hep-th/0306194](#)].
- [34] D. Anninos, *De Sitter Musings*, *Int. J. Mod. Phys. A* **27** (2012) 1230013, [[1205.3855](#)].
- [35] G. Dvali, *Black Holes and Large N Species Solution to the Hierarchy Problem*, *Fortsch. Phys.* **58** (2010) 528–536, [[0706.2050](#)].

- [36] R. Bousso and S. W. Hawking, *Pair creation of black holes during inflation*, *Phys. Rev. D* **54** (1996) 6312–6322, [[gr-qc/9606052](#)].
- [37] M. Spradlin, A. Strominger and A. Volovich, *Les Houches lectures on de Sitter space*, in *Les Houches Summer School: Session 76: Euro Summer School on Unity of Fundamental Physics: Gravity, Gauge Theory and Strings*, pp. 423–453, 10, 2001. [hep-th/0110007](#).
- [38] M. R. Visser, *Emergent gravity in a holographic universe*. PhD thesis, Amsterdam U., 2019. [1908.05469](#).
- [39] R. M. Wald, *Black hole entropy is the Noether charge*, *Phys. Rev. D* **48** (1993) R3427–R3431, [[gr-qc/9307038](#)].
- [40] T. Jacobson, G. Kang and R. C. Myers, *On black hole entropy*, *Phys. Rev. D* **49** (1994) 6587–6598, [[gr-qc/9312023](#)].
- [41] T. Banks, *Some thoughts on the quantum theory of stable de Sitter space*, [hep-th/0503066](#).
- [42] M. K. Parikh and E. P. Verlinde, *De Sitter holography with a finite number of states*, *JHEP* **01** (2005) 054, [[hep-th/0410227](#)].
- [43] D. Anninos, S. A. Hartnoll and D. M. Hofman, *Static Patch Solipsism: Conformal Symmetry of the de Sitter Worldline*, *Class. Quant. Grav.* **29** (2012) 075002, [[1109.4942](#)].
- [44] D. Anninos and D. M. Hofman, *Infrared Realization of dS_2 in AdS_2* , *Class. Quant. Grav.* **35** (2018) 085003, [[1703.04622](#)].
- [45] S. Leuven, E. Verlinde and M. Visser, *Towards non-AdS Holography via the Long String Phenomenon*, *JHEP* **06** (2018) 097, [[1801.02589](#)].
- [46] E. Coleman, E. A. Mazenc, V. Shyam, E. Silverstein, R. M. Soni, G. Torroba et al., *de Sitter Microstates from $T\bar{T} + \Lambda_2$ and the Hawking-Page Transition*, [2110.14670](#).
- [47] L. Susskind, *De Sitter Holography: Fluctuations, Anomalous Symmetry, and Wormholes*, *Universe* **7** (2021) 464, [[2106.03964](#)].
- [48] L. Susskind, *Black Holes Hint Towards De Sitter-Matrix Theory*, [2109.01322](#).
- [49] E. Shaghoulian, *The central dogma and cosmological horizons*, [2110.13210](#).
- [50] T. Banks, B. Fiol and A. Morisse, *Towards a quantum theory of de Sitter space*, *JHEP* **12** (2006) 004, [[hep-th/0609062](#)].
- [51] T. Banks and W. Fischler, *Holographic Space-time, Newton’s Law and the Dynamics of Black Holes*, [1606.01267](#).
- [52] T. Banks, W. Fischler, S. H. Shenker and L. Susskind, *M theory as a matrix model: A Conjecture*, *Phys. Rev. D* **55** (1997) 5112–5128, [[hep-th/9610043](#)].
- [53] S. R. Coleman and F. De Luccia, *Gravitational Effects on and of Vacuum Decay*, *Phys. Rev. D* **21** (1980) 3305.
- [54] R. Gregory, I. G. Moss and B. Withers, *Black holes as bubble nucleation sites*, *JHEP* **03** (2014) 081, [[1401.0017](#)].
- [55] J. Cotler and K. Jensen, *Gravitational Constrained Instantons*, *Phys. Rev. D* **104** (2021) 081501, [[2010.02241](#)].

- [56] P. Draper and S. Farkas, *de Sitter black holes as constrained states in the Euclidean path integral*, *Phys. Rev. D* **105** (2022) 126022, [[2203.02426](#)].
- [57] A. Strominger, *The dS / CFT correspondence*, *JHEP* **10** (2001) 034, [[hep-th/0106113](#)].
- [58] E. Witten, *Quantum gravity in de Sitter space*, in *Strings 2001: International Conference*, 6, 2001. [hep-th/0106109](#).
- [59] J. M. Maldacena, *Non-Gaussian features of primordial fluctuations in single field inflationary models*, *JHEP* **05** (2003) 013, [[astro-ph/0210603](#)].
- [60] M. Alishahiha, A. Karch, E. Silverstein and D. Tong, *The dS/dS correspondence*, *AIP Conf. Proc.* **743** (2004) 393–409, [[hep-th/0407125](#)].
- [61] M. Alishahiha, A. Karch and E. Silverstein, *Hologravity*, *JHEP* **06** (2005) 028, [[hep-th/0504056](#)].
- [62] X. Dong, E. Silverstein and G. Torroba, *De Sitter Holography and Entanglement Entropy*, *JHEP* **07** (2018) 050, [[1804.08623](#)].
- [63] V. Gorbenko, E. Silverstein and G. Torroba, *dS/dS and $T\bar{T}$* , *JHEP* **03** (2019) 085, [[1811.07965](#)].
- [64] M. Van Raamsdonk, *Cosmology from confinement?*, *JHEP* **03** (2022) 039, [[2102.05057](#)].
- [65] G. Araujo-Regado, R. Khan and A. C. Wall, *Cauchy Slice Holography: A New AdS/CFT Dictionary*, [2204.00591](#).
- [66] A. Almheiri, R. Mahajan, J. Maldacena and Y. Zhao, *The Page curve of Hawking radiation from semiclassical geometry*, *JHEP* **03** (2020) 149, [[1908.10996](#)].
- [67] H. Z. Chen, R. C. Myers, D. Neuenfeld, I. A. Reyes and J. Sandor, *Quantum Extremal Islands Made Easy, Part II: Black Holes on the Brane*, *JHEP* **12** (2020) 025, [[2010.00018](#)].
- [68] J. Hernandez, R. C. Myers and S.-M. Ruan, *Quantum extremal islands made easy. Part III. Complexity on the brane*, *JHEP* **02** (2021) 173, [[2010.16398](#)].
- [69] J. Maldacena, *Vacuum decay into Anti de Sitter space*, [1012.0274](#).
- [70] J. L. F. Barbon and E. Rabinovici, *Holography of AdS vacuum bubbles*, *JHEP* **04** (2010) 123, [[1003.4966](#)].
- [71] J. L. F. Barbon and E. Rabinovici, *AdS Crunches, CFT Falls And Cosmological Complementarity*, *JHEP* **04** (2011) 044, [[1102.3015](#)].
- [72] K. Skenderis and B. C. van Rees, *Real-time gauge/gravity duality*, *Phys. Rev. Lett.* **101** (2008) 081601.
- [73] K. Skenderis and B. C. van Rees, *Real-time gauge/gravity duality: Prescription, Renormalization and Examples*, *JHEP* **05** (2009) 085.
- [74] M. Botta-Cantcheff, P. Martínez and G. A. Silva, *On excited states in real-time AdS/CFT*, *JHEP* **02** (2016) 171, [[1512.07850](#)].
- [75] L. J. Romans, *Supersymmetric, cold and lukewarm black holes in cosmological Einstein-Maxwell theory*, *Nucl. Phys. B* **383** (1992) 395–415, [[hep-th/9203018](#)].
- [76] I. S. Booth and R. B. Mann, *Cosmological pair production of charged and rotating black holes*, *Nucl. Phys. B* **539** (1999) 267–306, [[gr-qc/9806056](#)].

- [77] J. McInerney, G. Satishchandran and J. Traschen, *Cosmography of KNdS Black Holes and Isentropic Phase Transitions*, *Class. Quant. Grav.* **33** (2016) 105007, [[1509.02343](#)].
- [78] A. Climent, R. Emparan, R. Hennigar and Q. Llorens., *In preparation*.
- [79] G. W. Gibbons and S. W. Hawking, *Action Integrals and Partition Functions in Quantum Gravity*, *Phys. Rev. D* **15** (1977) 2752–2756.
- [80] B. Banihashemi and T. Jacobson, *Thermodynamic ensembles with cosmological horizons*, [2204.05324](#).
- [81] J. W. York, *Black-hole thermodynamics and the euclidean einstein action*, *Phys. Rev. D* **33** (Apr, 1986) 2092–2099.
- [82] R. Emparan, A. M. Frassino, M. Sasieta and M. Tomašević, *Holographic complexity of quantum black holes*, *JHEP* **02** (2022) 204, [[2112.04860](#)].
- [83] A. Reynolds and S. F. Ross, *Complexity in de Sitter Space*, *Class. Quant. Grav.* **34** (2017) 175013, [[1706.03788](#)].
- [84] S. Chapman, D. A. Galante and E. D. Kramer, *Holographic complexity and de Sitter space*, *JHEP* **02** (2022) 198, [[2110.05522](#)].
- [85] E. Jørstad, R. C. Myers and S.-M. Ruan, *Holographic complexity in dS_{d+1}* , *JHEP* **05** (2022) 119, [[2202.10684](#)].
- [86] J. F. Pedraza, A. Russo, A. Svesko and Z. Weller-Davies, *Lorentzian Threads as Gatelines and Holographic Complexity*, *Phys. Rev. Lett.* **127** (2021) 271602, [[2105.12735](#)].
- [87] J. F. Pedraza, A. Russo, A. Svesko and Z. Weller-Davies, *Sewing spacetime with Lorentzian threads: complexity and the emergence of time in quantum gravity*, *JHEP* **02** (2022) 093, [[2106.12585](#)].
- [88] J. F. Pedraza, A. Russo, A. Svesko and Z. Weller-Davies, *Computing spacetime*, [2205.05705](#).
- [89] N. Bao, C. Cao, S. M. Carroll and A. Chatwin-Davies, *De Sitter Space as a Tensor Network: Cosmic No-Hair, Complementarity, and Complexity*, *Phys. Rev. D* **96** (2017) 123536, [[1709.03513](#)].
- [90] A. Almheiri, R. Mahajan and J. E. Santos, *Entanglement islands in higher dimensions*, *SciPost Phys.* **9** (2020) 001, [[1911.09666](#)].
- [91] T. Hartman, Y. Jiang and E. Shaghoulian, *Islands in cosmology*, *JHEP* **11** (2020) 111, [[2008.01022](#)].
- [92] L. Aalsma and W. Sybesma, *The Price of Curiosity: Information Recovery in de Sitter Space*, *JHEP* **05** (2021) 291, [[2104.00006](#)].
- [93] J. Kames-King, E. M. H. Verheijden and E. P. Verlinde, *No Page curves for the de Sitter horizon*, *JHEP* **03** (2022) 040, [[2108.09318](#)].
- [94] M. Casals, A. Fabbri, C. Martínez and J. Zanelli, *Quantum dress for a naked singularity*, *Phys. Lett. B* **760** (2016) 244–248, [[1605.06078](#)].
- [95] H.-J. Matschull, *Black hole creation in $(2+1)$ -dimensions*, *Class. Quant. Grav.* **16** (1999) 1069–1095, [[gr-qc/9809087](#)].

- [96] S. M. Christensen, *Vacuum Expectation Value of the Stress Tensor in an Arbitrary Curved Background: The Covariant Point Separation Method*, *Phys. Rev. D* **14** (1976) 2490–2501.
- [97] R. M. Wald, *Trace Anomaly of a Conformally Invariant Quantum Field in Curved Space-Time*, *Phys. Rev. D* **17** (1978) 1477–1484.
- [98] R. Herman and W. A. Hiscock, *Renormalization of the charged scalar field in curved space*, *Phys. Rev. D* **53** (1996) 3285–3295, [[gr-qc/9509015](#)].
- [99] D. Birmingham, *Topological black holes in Anti-de Sitter space*, *Class. Quant. Grav.* **16** (1999) 1197–1205, [[hep-th/9808032](#)].